The effect of size, morphology and surface properties of mesoporous silica nanoparticles on pharmacokinetic aspects and potential toxicity concerns

Uranous Niroumand[1], Negar Firouzabadi[2], Ghazal Goshtasbi[2], Bahareh Hassani[2], Parisa Ghasemiyeh[3,4] and Soliman Mohammadi-Samani [ID] [1,4,5]*

[1]Department of Pharmaceutical Nanotechnology, Shiraz University of Medical Sciences, Shiraz, Iran, [2]Department of Pharmacology and Toxicology, School of Pharmacy, Shiraz University of Medical Sciences, Shiraz, Iran, [3]Department of Clinical Pharmacy, School of Pharmacy, Shiraz University of Medical Sciences, Shiraz, Iran, [4]Pharmaceutical Sciences Research Center, Shiraz University of Medical Sciences, Shiraz, Iran, [5]Department of Pharmaceutics, School of Pharmacy, Shiraz University of Medical Sciences, Shiraz, Iran

Mesoporous silica nanoparticles (MSNs) are considered as suitable delivery vehicles considering their unique characteristics. Various physicochemical characteristics of MSNs govern their pharmacokinetic parameters which affect the disposition of these nanoparticles in the body. Along with the advantages of MSNs, the toxicity of nanoparticles entering the body is a major concern. Various factors such as particle size, surface charge, route of administration, *etc.*, may affect organ toxicity of MSNs. The main target organs involved in the metabolism and elimination of MSNs are the kidney and the liver as well as the hematopoietic system. In this review, we first introduced the physicochemical characteristics of MSNs which affect the pharmacokinetic properties including drug absorption and bio-distribution. Thereafter, we discussed the mechanisms by which organ toxicity may occur. In this regard, the effects of various factors on organ-based MSNs toxicities and molecular mechanisms have been summarized. At last, we emphasized on the role of the physicochemical parameters on organ-based toxicities, and the proposed approaches to prevent or at least diminish MSN-related toxicities are discussed in detail.

KEYWORDS

mesoporous silica nanoparticles (MSN), physicochemical factors, pharmacokinetics, hepatotoxicity, nephrotoxicity, hematotoxicity

1 Introduction

Mesoporous silica nanoparticles (MSNs) are well-ordered porous materials with a pore size range of 2 to 30 nm. MSNs were designed to carry the large molecules that cannot be incorporated within the micropores of conventional zeolites (SlowingVivero-Escoto et al., 2010). MSNs are a subset of colloidal silica, that soluble silica precursors are gathered into liquid-crystalline mesophases in the presence of amphiphilic surfactants or using block copolymers as structure-directing agents, based on the dominant detergent phase diagram. MSNs have been considered as potential nanocarriers which have gained much attention in

recent years for the treatment of a diverse set of illnesses, especially cancer. Easy functionalization, physicochemical stability, low toxicity, and great loading capacity propose MSNs as an attractive control drug delivery system (Manzano and Vallet-Regí, 2018). MSNs may be considered as promising nanocarriers for various therapeutic purposes due to their large surface area and also large pore sizes, appreciable physicochemical stability, high drug loading capacity, and controllable drug release properties (Sábio et al., 2021). In addition, functionalization of MSNs with desired moieties can lead to targeted delivery to the specific site of action (Li et al., 2012). Therefore, MSNs have found emerging applications in numerous fields especially nanotechnology, nanomedicine, and biomedicine for therapeutic, diagnostic, and theranostic purposes (Lee et al., 2011; Jafari et al., 2019).

Due to the tunable properties of MSNs as drug delivery systems, they can be administered through various routes including oral (Fang et al., 2023), topical, transdermal (Kolimi et al., 2023), parenteral, nasal, pulmonary, ophthalmic, and intra-tumoral (Sábio et al., 2021). However, intravenous (IV) and oral along with intraperitoneal (IP) administration are the main routes of administration of MSNs which determine the fate of these nanoparticles (NPs) including absorption, distribution, metabolism, and elimination. Numerous multifunctional MSNs have been designed with the aim of targeted delivery through the desired route of administration. Their main advantages would be enhanced cellular uptake, prolonged circulation time, and tunable drug release potential (Sábio et al., 2021).

Although MSNs have multiple biomedical applications, because of their unique physicochemical properties, there are concerns about their safety and potential toxicities (Fu et al., 2013; Karmakar et al., 2014; Mirshafiee et al., 2017; Baeza and Vallet-Regí, 2020; MacCuaig et al., 2022). Therefore, assessment of their safety is of great importance. Since there is not much information available on the toxicological outcome of MSNs, the application of MSNs in drug delivery has faced many challenges (Rascol et al., 2018). Hence, evaluation and assessment of the mechanisms of nephrotoxicity and hepatotoxicity and the need to provide methods or pharmacological interventions to prevent organ toxicities caused by MSNs are of great concern (Wang et al., 2022).

Physicochemical properties of MSNs including their particle size (He et al., 2011), pore size (Zhang et al., 2012), shape and morphology (Huang et al., 2011), specific surface area and surface charge (Chung et al., 2007), and functionalization (Peng et al., 2022) can highly affect their fate and pharmacokinetic aspects including bio-distribution and clearance after the administration through various routes. In this regard, this review mainly focused on the effect of each of these physicochemical factors on MSNs pharmacokinetic and also MSN-related toxicities, especially MSN-associated nephrotoxicity, hepatotoxicity, and hematotoxicity. In this review, we first introduced various physicochemical properties of MSNs including their particle size, particle shape, mesoporosity, pore size, specific surface area and surface charge, and also surface functionalization. Since MSNs can significantly affect the blood circulation time of the loaded cargo (Peng et al., 2020) and also since the two main organs of clearance are the kidney and the liver, we thereafter, emphasized on the molecular mechanisms involved in the hepatotoxicity, nephrotoxicity, and hematotoxicity of MSNs and propose

molecular interventions in prevention and management of their possible associated toxicities. Finally, the effect of MSNs functionalization and also their unique physicochemical properties in the induction and avoidance of these potential toxicities are summarized and discussed in detail.

2 Effects of physicochemical factors on pharmacokinetic parameters

2.1 Particle size

Particle size that is defined as the diameter or dimension of the particles can highly affect the MSNs' fate in the body. MSNs with a hydrodynamic diameter of smaller than 100 nm have higher delivery efficiencies than larger ones. Furthermore, nearly neutral charged NPs (with zeta potential values of about −10 to +10 mV) have higher delivery efficiencies than those with higher zeta potential values. In addition, rod-shaped NPs are more efficient for drug delivery purposes than spherical or flake-like ones. These trends probably reflect the *in vivo* stabilities of the NPs and differences in renal clearance. Previous bio-distribution studies have shown that physicochemical properties of NPs including particle size, particle charge, and surface polymeric coatings (He et al., 2011; Meng et al., 2011; Chen et al., 2013) along with routes of administration (Garbuzenko et al., 2014; Sapino et al., 2015; Lindén, 2018) are critical in governing the fate of NPs. However, systematic comparisons are lacking.

As mentioned previously, particle size would be crucial for designing a topical drug delivery system. Results of a previous study using synthesized three silica particles (SP) with different particle sizes ranging from 400 to 600 nm (nSP), 2 μm (mSP-2), and 7 μm (mSP-7) for topical drug delivery of metronidazole, revealed that the depth of skin penetration through the human skin model was different. Therefore, these results revealed that the vertical distribution of these SPs was size-dependent. In this regard, the nano-sized silica particles (nSP) with particle size ranges of 400–600 nm were accumulated in the skin microstructures and resided in furrows as far down as 20 μm, whilst the micro-sized SPs (mSP-2 and mSP-7) were found to reside superficially (Valetti et al., 2021).

Another study on gelatin-coated mesoporous hollow silica nanospheres (GSN) with an average particle size of 140 nm as a nanocarrier for glimepiride delivery was accompanied by enhanced water solubility of the incorporated drug along with controlled release rate and longer drug accumulation at the target site. Glimepiride-GSNs showed 40% drug release at 1 h and more than 90% during 24 h. In addition, this study revealed that the T_{max}, mean residence time (MRT), and 24-h area under the curve (AUC_{0-24h}) values in glimepiride-GSNs were significantly higher than the commercially available product counterparts. Moreover, the bioavailability of glimepiride was enhanced after incorporation into the GSNs and also lead to higher cellular and intestinal mucosal uptake (Yu et al., 2020).

A study on Nimesulide, a poorly water-soluble drug, loaded into chiral mesoporous silica nanoparticles (CMSN) and enlarged chiral mesoporous silica nanoparticles (E-CMSN) with a particle size range of 200 to 300 nm revealed that the E-CMSN was the

superior nanocarrier for NMS delivery due to its higher oral bioavailability and anti-inflammatory effects. Also, the E-CMSN with enlarged mesoporous characteristics showed higher drug loading capacity (Guo et al., 2019).

The potential effect of particle size on bio-distribution and drug clearance kinetics has been studied in healthy rats using stable, monosized, and radiolabeled MSNs. Results revealed that increasing the particle size from ~32 nm to ~142 nm was accompanied by a monotonic decrease in systemic bioavailability irrespective of the route of drug administration due to higher accumulation in the liver and spleen (Dogra et al., 2018). Results of another study on the bio-distribution and excretion of MSNs and polyethylene glycol (PEG)-MSNs with different particle size ranges (80, 120, 200, and 360 nm) on the animal model through tail-vein injection revealed that PEG-MSNs in comparison to the MSNs with the same particle size had much lower liver, spleen, and lung uptake which lead to lower bio-distribution concentrations and therefore longer systemic circulation life-time, slower biodegradation, and lower excretion rate of the degradation products. In addition, the results of this study revealed that MSNs with small particle sizes could easily escape from the liver and spleen uptakes, therefore, slower biodegradation and much lower excretion rate of biodegradation products were obtained (He et al., 2011). In another study, MSNs coated with pH-responsive poly (N-isopropylacrylamide-co-methacrylic acid; P NIPAM-co-MAA) for doxorubicin (DOX) delivery (P-MSN-DOX) were fabricated. Based on the obtained results, P-MSN-DOX NPs with a particle size of 190 ± 30 nm and loading capacity of more than 20%, had longer systemic circulation along with lower cardiac and renal drug accumulation and therefore much lower organ toxicity. A Pharmacokinetic study showed that P-MSN-DOX had a larger AUC value and longer half-life in comparison to the free DOX. Also, the free DOX was rapidly eliminated from systemic circulation. In contrast, MSN-DOX and P-MSN-DOX delivery systems showed noticeably delayed and reduced drug clearance (Chen et al., 2013).

Pharmacokinetic study on paclitaxel and curcumin-loaded homogeneous PEGylated lipid bilayers coated with highly ordered MSNs (PLMSNs) with a particle size of 115 ± 15 nm and thickness of 10–15 nm suggested that this novel drug delivery system could significantly enhance the AUC of both encapsulated drugs. In addition, the half-life of paclitaxel in the PLMSNs group was 7.2-fold higher than that of the free paclitaxel. As a result, longer systemic circulation could be achieved. Also, the C_{max} of both paclitaxel and curcumin in PLMSNs group was much higher than that of the free drug group (Gao et al., 2019).

Skin penetration and cellular uptake of the amorphous SPs with particle sizes ranging from 291 ± 9 nm to 42 ± 3 nm were also investigated. NPs were applied on human skin explants with partially disrupted stratum corneum. Results revealed that only the SPs with an average diameter of 42 ± 3 nm are capable of penetrating the epidermal cells and especially dendritic cells. Therefore, skin penetration of these SPs was size-dependent. It has been reported that NPs with an average diameter of above 75 nm were unable to penetrate through the human skin even after mild skin barrier disruption by means of cyanoacrylate biopsy (Rancan et al., 2012).

Comparison among three different DOX-loaded MSNs including non-coated (NP1, 100 nm), PEG-coated (NP2, 50 nm), and PEI-PEG-coated (NP3, 50 nm) NPs revealed that particle size

reduction and surface functionalization of MSNs was accompanied with diminished particles opsonization and enhanced passive delivery of DOX to human squamous carcinoma xenograft in nude mice after IV injection. In addition, results of this study showed that MSNs with an average particle size of 50 nm coated with PEI-PEG copolymer were capable to obtain an excellent EPR effect in comparison with the non-coated larger ones (NP1, 100 nm) or those coated with PEG alone (NP2, 50 nm) confirming the effect of surface functionalization (Meng et al., 2011).

Altogether, MSNs with smaller particle sizes show enhanced skin penetration, better cellular uptake, reduced nanoparticles opsonization, longer circulation time, reduced drug accumulation within the organs and therefore diminished related toxicities, longer half-lives, and more controllable drug release profile.

2.2 Mesoporosity and pore size

A mesoporous material is a nanoporous material containing pores with a diameter between 2 and 50 nm. Fabrication of MSNs should be accompanied by managing their pore sizes, since pore size would be an essential physicochemical property of MSNs that can affect the amount of drug loading and also dug release profile. In order to assess the effect of the MSNs' pore size on the release pattern of poorly water-soluble drugs including itraconazole, pore size was enhanced from 4.5 nm to 6.4 nm and the results suggested a significant increase in drug release rate. While further enhancement in MSNs' pore size from 7.9 nm to 9 nm was accompanied by only a minor enhancement in drug release rate emphasizing on the effect of critical MSNs' pore size on molecular diffusion and drug release rate. Therefore, it seems that itraconazole release profile from MSNs can be tuned through alteration in pore sizes of NPs to optimum values in order to obtain the desired kinetics of drug release (Mellaerts et al., 2007).

Results of another study on captopril-loaded MSNs recruiting three different surfactants including C16TAB, C12TAB, and EO20PO70EO20 revealed that through pore sizes increase, the drug loading amount enhances significantly. In addition, MSNs with the largest pore size (7.39 nm) showed the fastest drug release rate (Qu et al., 2006).

In another study, fenofibrate-loaded three-ordered MSNs with different pore diameters including 7.3 nm, 4.4 nm, and 2.7 nm were designed and compared. Results revealed a significant increase in drug release rate with increasing the pore sizes of MSNs. While the pharmacokinetic data of this study showed that MSNs with smaller pore sizes had better therapeutic efficacies with larger AUC values (Van Speybroeck et al., 2010).

Another study investigated the effect of MCM-48 with pore sizes of 3.7 nm and SBA-15 with pore sizes of 8.8 nm on the release kinetics of ibuprofen. Results showed that pore sizes of MSNs can affect drug release profile and its kinetic. In this regard, drug release kinetics was best fitted with first-order and zero-order kinetics for MCM-48 and SBA-15, respectively (Izquierdo-Barba et al., 2009).

Raloxifene hydrochloride with limited aqueous solubility was incorporated into MSNs (with different pore sizes) including RLF-41 (3.11 nm), RLF-48 (2.5 nm), RLF-41-NH2 (2.96 nm), and RLF-48-NH2 (2.3 nm) in order to enhance its bioavailability. Results of this study revealed that the C_{max} values gradually declined in the

following order: RLF-48< RLF-41<RLF-48-NH2<RLF-41-NH2. In addition, the enhanced water solubility and systemic bioavailability were more obvious for RLF-48 and RLF-48-NH in comparison to RLF-41 and RLF-41-NH2 (Shah and Rajput, 2019).

Ibuprofen, a poorly aqueous-soluble drug, was co-spray dried with MSNs (with different pore sizes) including MCM-41 (2 nm), SBA-15 (6–8 nm), and SBA-15-LP (20 nm) in order to enhance the dissolution rate. Results suggested that the physical and solid state of ibuprofen were also affected by the pore sizes of MSNs. Nanocrystalline ibuprofen could be incorporated into the pore channels of ≥20 nm in diameter, while the amorphous ibuprofen could be incorporated into the pore sizes of <10 nm. Therefore, the dissolution rate could be affected by the solid state of the drug and also the pore sizes of MSNs. The dissolution rate of co-spray dried ibuprofen/SBA-15 was relatively faster than that of ibuprofen/ MCM-41 with percentage values of 95% vs. 88%, respectively during 15 min. The dissolution rate of ibuprofen in ibuprofen/ SBA-15-LP formulation with pore sizes of 20 nm was the slowest with 76% dissolution during 15 min (Shen et al., 2011).

Cilostazol-loaded into two different MSNs including MCM-41 and MCM-48 was designed to enhance the systemic bioavailability of cilostazol. Results revealed that cilostazol-loaded MSNs with different specific surface area pore sizes (surface area of 978.66 m^2/g and pore size 3.8 nm for MCM-41 and surface area of 1108.04 m^2/g and pore size of 3.6 nm for MCM-48) showed different behaviors in adsorption. The cumulative percentages of drug release from cilostazol-MCM-48 and cilostazol-MCM-41 within 60 min were 63.41% and 85.78%, respectively. While the cumulative percentages of drug release within 12 h reached 100% for both of these MSNs. The dissolution rate, C_{max}, and AUC values were significantly enhanced in MSNs formulation in comparison to the free cilostazol. According to the results of drug release assessments, MCM-41 with a pore size of 3.8 nm would be a potential nanocarrier for sustained drug release purposes due to its longer disconnected tubular structure. Results of the pharmacokinetic assay revealed that both MSNs, especially the MCM-48 formulation, could significantly improve the bioavailability of cilostazol (Wang et al., 2014).

In a study, ibuprofen-loaded three-ordered MSNs were synthesized inside the channels (120–200 nm in diameter and 60 µm long) of porous anodic alumina membranes with different pore sizes including COL-CTAB (4.73 nm), CIRC-P123 (6.08 nm), and COL-P123 (6.32 nm) and the effect of MSNs' pore size on the loading and release pattern of ibuprofen was investigated. According to the reported data, ibuprofen in COL-P123 formulation had the highest loading levels. Therefore, in MSNs with columnar morphology, there was a significant association between pore diameter and drug adsorption or loading capacity within the mesoporous structure. MSNs with limited pore access showed much lower drug adsorption within the NPs. In addition, the morphology and pore sizes of the MSNs could drastically affect the drug release rate. In this regard, results revealed that in columnar MSNs, an increase in pore diameter could significantly enhance the drug release rate (Cauda et al., 2009).

Taken together, MSNs with larger pore sizes promote faster release rates. In addition, the pore size of MSNs could significantly affect the kinetics of the drug release profile. Furthermore, MSNs with larger pore sizes show faster dissolution rates of loaded compounds in comparison to those with smaller pore sizes.

2.3 Shape and morphology

In order to show the crucial effect of MSNs' shape on the pharmacokinetics profile of the loaded drugs, three different shapes of nifedipine-loaded fluorescent MSNs including long rod NPs (NLR), short rod NPs (NSR), and spherical NPs (NS) were investigated in a study after oral administration. Results of animal studies indicated that the rod NPs had a longer residence time in the gastrointestinal tract in comparison with the spherical ones. In addition, the capability of NLR to overcome the rapid clearance through the reticuloendothelial system (RES) was greater in comparison with NSR and NS. Therefore, NLR exhibited a longer systemic circulation than NSR and NS. Furthermore, spherical NPs were cleared faster than rod ones through renal excretion. Also, MSNs with different shapes showed different biodegradation rates. In this regard, NSR had faster degradation than NLR and NS. Results of the pharmacokinetic study demonstrated that nifedipine-loaded NLR had a higher bioavailability than NSR and NS formulations. In addition, the $AUC_{0-\infty}$ of -loaded NLR, nifedipine-loaded NSR, and nifedipine-loaded NS were 2.1-fold, 1.6-fold, and 1.4-fold higher than that of the commercially available nifedipine tablets, respectively. T_{max}, the time taken to reach C_{max} was about 10 min for all three MSNs, while it was about 30 min for commercial nifedipine tablets (Zhao et al., 2017).

The capability of albumin-coated hollow MSNs (A-HMSNs) to improve the chemotherapeutic efficacy of docetaxel was investigated in previous studies. Based on the results, A-HMSNs could significantly improve the pharmacokinetic profile of docetaxel in comparison with the free drug. Increased C_{max}, T_{max}, MRT, and AUC values, prolonged drug release, extended systemic circulation time, lower drug clearance, hemocompatibility, and higher drug loading capacities were observed with this nano-delivery system. Notably, these A-HMSNs were spherical in shape and had hollow structures (Pandita et al., 2021).

Another study, investigated the effect of MSNs' shape on oral delivery and bioavailability of indomethacin, mesoporous silica nanorods (MSNRs), and mesoporous silica nanospheres (MSNSs). Results revealed that the cumulative percentage of drug release from MSNRs reached 100% after 1 h, while this percentage for free drug was only 27% after 1.5 h. The dissolution rate of indomethacin in MSNRs was faster than that of MSNSs. Therefore, different dissolution rates might be attributed to different pore architectures and shapes of the MSNs. Since the MSNRs had relatively more ordered helical channels and larger pore sizes in their structure than MSNSs, therefore faster dissolution rate of indomethacin was achieved with MSNRs. In addition, the bioavailability of indomethacin-MSNR was approximately 4-fold and 2.2-fold higher than that of the free indomethacin solution and indomethacin-MSNS. Similarly, the AUC of indomethacin-MSNR was significantly higher than that of indomethacin-MSNS and free indomethacin solution (1.3-fold and 2.2-fold, respectively). Moreover, MSNRs showed a longer systemic circulation and could more easily overcome the rapid clearance through RES in comparison with the MSNSs (Zhang et al., 2018a).

DOX hydrochloride DOX-loaded MSNSs and MSNRs with different aspect ratios but identical surface chemistry were designed to investigate the effect of MSNs' shape on oral

delivery. The results of this study revealed that MSNRs had a higher cellular uptake than MSNSs. The apparent permeability coefficient value of DOX-loaded MSNRs was about 1.8-fold, 3.2-fold, and 6.3-time higher than DOX-loaded MSNS1, DOX-loaded MSNS2, and free DOX solution, respectively. Also, the results of *in vivo* pharmacokinetics study indicated that the AUC of DOX-loaded MSNRs was 1.9-fold, 3.4-fold, and 5.7-fold higher than that of DOX-loaded MSNS1, DOX-loaded MSNS2, and free DOX solution, respectively (Zheng et al., 2018).

Another study investigated the effect of spherical and rod-shaped mesoporous structures on cellular uptake efficiency in various cancerous cell lines for potential uses as nanomedical drug delivery systems. On the other hand, rod-shaped and spherical particles were easily uptake by HeLa cells with minor shape and charge differences, while in the Caco-2 cells, rod-shaped particles were uptake more easily than spherical ones (Karaman et al., 2012).

Three PEGylated fluorescent MSNs (FMSN-PEG) with different shapes including long-rod (NLR-PEG), short-rod (NSR-PEG), and sphere (NS-PEG) NPs were fabricated to evaluate the effect of NPs shape on the cellular uptake pathway in Hela cells. The cellular uptake kinetics and the pathways of these three different FMSN-PEG were completely shape-dependent. In this regard, the NLR-PEG showed higher intracellular retention amounts than the NSR-PEG and NS-PEG over 8 h. The NSR-PEG showed the lowest intracellular retention amount, especially with prolonged incubation time. It has been reported that spherical NPs were preferred in terms of internalization through the clathrin-mediated pathway, while the MSNs with larger aspect ratios were preferred to be internalized through the caveolae-mediated pathway. Therefore, different cellular uptake kinetics can be attributed to the different shapes of MSNs (Hao et al., 2012).

Furthermore, two different shapes of fluorescent MSNs with AR values of 1.5, and 5 were designed in another study to investigate the effects of NPs shape on bio-distribution, clearance, and biocompatibility of the drugs through *in vivo* studies. Results revealed that short-rod MSNs were easily uptake and trapped within the liver, while long-rod MSNs were more distributed in the spleen. Also, the clearance of MSNs was primarily dependent on the nanoparticles' shape. In this regard, the short-rod MSNs had a more rapid clearance than long-rod ones (Huang et al., 2011).

In summary, Rod shape MSNs have longer residence time in the gastrointestinal tract in comparison with the spherical ones. In addition, the long rod MSNs have a greater capability to overcome the rapid clearance through the RES in comparison with the short rod MSNs and spherical ones. Therefore, long rod MSNs exhibit a longer systemic circulation than short rod and spherical shape MSNs. Moreover, spherical MSNs show faster renal clearance than rod-shaped ones. The dissolution rate of loaded drugs in nanorod MSNs is faster than that of nanosphere MSNs.

2.4 Surface functionalization

Surface functionalization can be defined as the decoration of different functional groups, via the chemical bonds, on the surface of the particles. In a study, resveratrol, a polyphenol agent with anti-oxidant, anti-inflammatory, and anti-cancer properties, was loaded into the uniformly sized (~60 nm) functionalized MSNs including PO_3-MSNs and NH_2-MSNs in order to improve its *in vitro* anti-proliferative activity and also to sensitize docetaxel in hypoxia-induced drug resistance in prostate cancer. Resveratrol was efficiently encapsulated within phosphonate (PO_3; negatively charged) and amine (NH_2; positively charged)-decorated MSNs. The effect of surface functionalization of MSNs on drug loading, *in vitro* drug release, anti-proliferative activity, and cytotoxic capability of resveratrol in prostate cancer cell lines was also investigated in this study. Results revealed that at pH 7.4, both free resveratrol and resveratrol-loaded NH_2-MSNs had burst drug release which reached to plateau (90% cumulative drug release) within 12 h, while the resveratrol-loaded PO_3-MSNs revealed a significantly slower drug release rate with only 50% cumulative drug release after 12 h. Drug release assessments at pH 5.5 showed that both PO_3-MSNs and NH_2-MSNs had sustained drug release over 24 h (about 40% cumulative drug release) (Chaudhary et al., 2019).

Oral administration of some nanocarriers still faced significant challenge in pharmaceutical industries. Since the designed nanocarriers should efficiently overcome multiple gastrointestinal barriers including the harsh gastrointestinal environment, the mucosal layer, and the epithelium layer. Neutral hydrophilic surfaces are necessary for mucosal permeation, while hydrophobic and cationic surfaces are crucial for efficient epithelial permeation. In order to adjust these conflicting surface properties, some strategies have been considered to modify nanocarriers surfaces. Surface modification with cationic cell-penetrating peptides concealed by a hydrophilic succinylated casein layer was one of these approaches. Furthermore, quantum dots doped hollow silica nanoparticles (HSQN) with an average diameter of about 180 nm were used and demonstrated a suitable loading efficacy of 50% for paclitaxel as a poorly water-soluble drug with low permeability. After gastrointestinal degradation of succinylated casein by peptidase, strong interaction with epithelial membranes led to a 5-time increase in cellular internalization. Results of the pharmacokinetics study on paclitaxel-loaded surface-modified MSNs revealed a 40% enhancement in absolute bioavailability and a 7.8-fold higher AUC value in comparison to the free paclitaxel after oral administration (Wang et al., 2018).

Indomethacin-loaded amino-modified mesoporous silica xerogel (B-AMSX) and mesoporous silica xerogel without amino modification (B-MSX) were designed in a study and characterized to improve drug solubility. Loading capacity of B-AMSX was higher than that of B-MSX. Since more indomethacin molecules can be encapsulated via the stronger hydrogen bonding force induced by the amine functional group. In addition, results of *in vitro* drug release assessment revealed that both B-MSX and B-AMSX could improve indomethacin release profile. However, indomethacin was released from the B-AMSX a little faster than the B-MSX due to the larger pore sizes in the B-AMSX structure (Li et al., 2016a).

A dual-functionalized MSN with carboxyl modification and chirality was successfully designed and developed for the purpose of DOX delivery. Characteristics of Dual-MSN and recruiting as DOX nanocarrier were compared with naked non-functionalized MSN. Results of this study indicated that both naked MSN and dual-MSN

could remarkably control DOX release because of the presence of release modulation induced by their mesoporous structure. However, the dual-MSN showed a pH-responsive drug release pattern due to the negative charges of its carboxyl groups. The cytotoxicity profile of DOX-loaded dual-MSN was better than DOX-loaded naked MSN owing to its enhanced cellular internalization governed by the chirality of dual-MSN. In addition, the outcome of this study emphasized on the superiority of dual-MSN in the enhancement of the antitumor effect of DOX against MCF-7 cells. Therefore, dual-MSN would be a promising nanocarrier for DOX delivery (Li et al., 2016b).

Curcumin-loaded amine-functionalized MSN was investigated to enhance the bioavailability of curcumin in animal models after oral administration. In this regard, the effect of particle size on drug release profile, drug solubility, and oral bioavailability of curcumin was assessed in both amine-functionalized MSN with particle size ranges of 100–200 nm and amine-functionalized mesoporous silica microparticles (MSM). Results revealed that curcumin-loaded amine-functionalized MSN (MSN-A-Cur) had a modified drug release pattern and enhanced drug solubility in comparison with curcumin-loaded amine-functionalized MSM (MSM-A-Cur). In addition, the bioavailability of both MSN-A-Cur and MSM-A-Cur were significantly higher than the free curcumin. These results confirmed the capability of amine-functionalized MSN as a preferred nanocarrier for oral delivery of poorly water-soluble drugs (Hartono et al., 2016).

Etoposide-loaded highly ordered hexagonal MSNs (MCM-41) and also MSNs functionalized with amino groups (MCM-41-A) were designed to assess the effect of amine-functionalization on the release pattern of poorly water-soluble drugs including etoposide. The release pattern of crystalline etoposide, commercial formulation, etoposide-MCM-4, and etoposide-MCM-41-A were assessed and compared. Drug release rate from MCM-41 was much faster than that of crystalline etoposide and commercial formulation. These results might be attributed to the enhanced dissolution rate of etoposide from MCM-41 of about 5.1-fold and 1.16-fold in comparison to the crystalline etoposide and commercial formulation, respectively. Furthermore, burst release was solely detected in unmodified MCM-41 NPs and it did not occur for MCA-41-A NPs. Drug release kinetics for MCM-41 and MCM-41-A NPs were best fitted with Weibull and Higuchi model, respectively. Therefore, the amine-functionalization of MSNs was accompanied by a more sustained drug release pattern (Saroj and Rajput, 2018).

In another study, DOX-loaded amino-modified multimodal MSNs (M-NSNs-NH_2) were fabricated to enhance drug loading capacity in order to obtain a controlled drug release profile. Results revealed that both M-NSNs and M-MSNs-NH_2 could significantly control the DOX release in comparison to free DOX. However, DOX-loaded M-MSNs-NH_2 showed a slower and more sustained drug release pattern in comparison to DOX-loaded M-MSNs which can be attributed to the presence of stronger hydrogen bonding forces between DOX and amine group in M-MSNs-NH_2 (Wang et al., 2017).

Paracetamol as the most commonly used analgesic and antipyretic drug has a challenge of dosing frequency. Therefore, it would be desirable to change the drug release kinetics to a zero-order model. In this regard, non-toxic wrinkled mesoporous carbons with specific morphology was fabricated as suitable carriers for paracetamol delivery. The fabricated particles could significantly control the release rate of the loaded drug over 24 h in a simulated gastric fluid and drug release kinetics was best fitted to the zero-order model. This delivery system could also increase the bioavailability of paracetamol and extend its duration of action (Goscianska et al., 2021). This study revealed that among the three different carriers including wrinkled mesoporous silica (WMS), wrinkled mesoporous carbon (WMC), and modified WMC (ox-WMC; oxidized with ammonium persulfate solution to produce surface oxygen-containing functional groups) which were investigated in paracetamol delivery, Ox-WMC had the lowest pore volume and average pore diameter in comparison with WMS and WMC. Hence, drug molecules could not be readily placed within the pores of ox-WMC and therefore paracetamol release pattern was faster than that of the non-functionalized WMC. Drug release assessment at pH 1.2 (simulated gastric fluid) revealed that the cumulative percentage of paracetamol release during 24 h was the highest for ox-WMC and the lowest for WMS. The initial burst release was only reported for WMS. The release rate of paracetamol from both WMC and ox-WMC remained constant over the assay period and no burst release occurred (Goscianska et al., 2021).

To obtain gemcitabine and quercetin delivery, MSN functionalized withNH_2, SH, and COOH, as suitable drug delivery systems were fabricated. Drug loading capacity and drug release profile of bare and functionalized MSNs were investigated for both gemcitabine (as a hydrophilic drug) and quercetin (as a hydrophobic drug). Based on the results, the functionalized MSNs exhibited higher drug loading capacity and slower drug release profile due to the electrostatic interaction and also the hydrogen bonding between the organic functional groups on the MSN surface and the drug molecules. Regarding quercetin, the MSN-NH_2 showed the highest drug loading (72%) and also the slowest pH-dependent drug release pattern. As for gemcitabine, the MSN-COOH showed the highest drug loading (45%) and also the slowest pH-dependent drug release (Zaharudin et al., 2020).

Results of another study reported that methotrexate delivery to the brain was significantly enhanced through the encapsulation of methotrexate in MSNs functionalized with transactivator of transcription peptide which is a cell-penetrating peptide. Therefore, surface functionalization of MSNs was accompanied by enhanced brain penetration and uptake, increased methotrexate half-life, and enhanced brain-to-plasma concentration ratios (Shadmani et al., 2023).

As a whole, Amine-functionalized MSNs with positive surface charge show a faster release rate in comparison to phosphate-functionalized MSNs with negative surface charge. However, the amino-functionalization of MSNs is accompanied by enhanced drug loading capacity and also a more sustained drug release pattern in comparison to the naked MSNs. Carboxyl-functionalized MSNs show a pH-responsive drug release pattern due to the negative charges of their carboxyl groups. In addition, carboxyl functionalization would be associated with enhanced cellular uptake of the loaded drug.

2.5 Specific surface area

Specific surface area is defined as the surface area of 1 g or 1 cm^3 of the materials. A study conducted on velpatasvir, a poorly water-soluble antiviral drug, was encapsulated into MSNs. In this regard, blank MSNs with specific surface area and pore diameter of 602.5 ± 0.7 m^2/g and 5.9 nm, were synthesized, respectively. The surface area and pore size values were reduced after the incorporation of velpatasvir into MSNs. The results of this study showed that free velpatasvir had a poor dissolution rate along with a progressive increase in the pH of the dissolution media that could reduce the oral bioavailability of velpatasvir. Drug release assessments at a wide range of pH values (from 1.2 to 6.8) revealed an enhancement in drug solubility and release pattern. In addition, the *in vivo* pharmacokinetic data showed that velpatasvir-MSNs could significantly enhance the oral bioavailability of the drug in comparison to free velpatasvir. Furthermore, the AUC and C_{max} values were enhanced for velpatasvir-MSNs, while the T_{max} was reduced in comparison to the free velpatasvir. The *in vivo* results were in accordance with the *in vitro* studies where the velpatasvir-MSNs in comparison to free velpatasvir showed rapid dissolution rate, higher absorption, higher systemic concentration, and higher accumulation of velpatasvir-MSNs at the target site, *i.e.,* the liver. Therefore, it seems that MSNs are capable of improving the both *in vitro* and *in vivo* performance of poorly water-soluble drugs with limited oral bioavailability (Mehmood et al., 2020).

Ibuprofen-loaded MSNs with specific microstructural properties were also synthesized through the binary surfactant templated approach with different concentrations of Pluronic F127. Results exhibited that the drug loading amount was mainly dependent on the specific surface area values. In this regard, the F127 concentration of 0.17 mM induced the highest specific surface area of 1300 m^2/g and the largest pore volume of 0.99 cm^3/g. While increment in the F127 concentrations was accompanied by a reduction in the specific surface area of MSNs. In general, the particle size reduction can increase the particle-specific surface area. It has been shown that the specific surface area of MSNs was profoundly affected by the NP's pore volume than the particle size, therefore, the highest surface area of MSNs was gained with the lowest F127 concentration. In addition, the amount of loaded drug was mostly dependent to the specific surface area. Also, the MSNs prepared with the highest F127 concentration showed the fastest drug release pattern (Chen et al., 2012).

All together, reduction in MSNs' particle sizes and also increase in porosity of MSNs are associated with enhanced surface area. In addition, the surface area of the MSNs is correlated with pore sizes. MSNs with higher surface area would result in a higher drug loading capacity and also a faster drug release rate.

2.6 Surface charge

Surface charge would be defined as density of the electric charge that existed on the surface of the particles. Porous silica particles with spherical and rod-shaped structures were investigated in a previous study to compare their cellular uptake efficiencies in 2 various cancerous cell lines including HeLa cells and Caco-2 cells. Based on the results, both of them could easily internalize into the HeLa cells with slight particle shape and particle charge differences. While, for Caco-2 cells, the rod-shaped particles could internalize more efficiently. The difference in cellular uptake was most obvious for uncoated silica particles for both HeLa and Caco-2 cell lines. In addition, it has been reported that silica particles with higher particle charges could induce higher cellular uptake. Therefore, a net positive charge could enhance cellular internalization regardless of particle shape and the type of cell line. Moreover, the surface charge is another potential factor to modulate the cellular internalization even in HeLa cells. It has been reported that higher particle charges (+/−) resulted in higher cellular uptake in comparison to the net neutral charge. However, the positive net charge was superior to the negative charge for the purpose of cellular uptake enhancement. At higher concentrations, the effect of surface charge was predominated in HeLa cells, and the rod-shaped particles were internalized regardless of coating. While for the sphere-shaped particles and Caco-2 cells, the distinctions based on particle coating still remained. Since the particle shape can influence the cellular uptake of drugs in a cell-dependent manner, morphologically engineered particles could be used potentially as a promising tool to enhance NP-mediated drug delivery (Karaman et al., 2012).

Two different indomethacin delivery systems including chiral MSNs (CMSNs with a surface area of 525.36 m^2/g) and amino-modified chiral MSNs (Amino-CMSNs with positive surface charge and surface area of 190.74 m2/g) were designed to assess the oral bioavailability and pharmacokinetic parameters. Both CMSN and Amino-CMSN were safe to be circulated in the blood. Also, the Amino-CMSN showed a significantly lower hemolysis ratio than CMSN. In addition, the oral bioavailability and anti-inflammation effect of indomethacin-loaded CMSN and Amino-CMSN were significantly enhanced in comparison to the free indomethacin which can be attributed to the enhanced dissolution rate. Moreover, the indomethacin-loaded Amino-CMSN with a positive surface charge could induce improved biological effects (Li et al., 2018).

Curcumin-loaded MSNs (MCM-41) with different surface chemistry properties were designed to assess the anticancer activity. Furthermore, curcumin encapsulated within pristine MCM-41 (a hydrophilic and negatively charged MSN), amino-functionalized MCM-41 (MCM-41-NH$_2$; a hydrophilic and positively charged MSN), and methyl-functionalized MCM-41 (MCM-41-CH$_3$; a hydrophobic and negatively charged MSN) were also synthesized, characterized and cell cytotoxicity was assessed in human squamous cell carcinoma (SCC25) cell line. Both positively and negatively charged hydrophilic MSNs were shown to improve drug release profiles and enhance anti-cancer activity in comparison to free curcumin. However, the positively charged hydrophilic MSNs showed higher cellular uptake in comparison to the negatively charged ones which can be attributed to the stronger electrostatic interactions with cells. The hydrophobic surface-modified NPs (MCM-41-CH3) showed no improvement in drug release profile, nor in its anticancer activity because of its poor wetting effect. Cell cycle analysis and cell apoptosis studies showed that although different mechanisms were involved in the anti-cancer properties of positively and negatively charged MSNs, they exhibited similar anti-cancer activity in SCC25 cells (Jambhrunkar et al., 2014).

Another study on large-pore Atto-647-MSNs with a hexagonal well-ordered pore structure was synthesized via sol-gel co-condensation of tetraethoxysilane and Atto-647-conjugated 3-aminopropyltrimethoxysilane in the presence of CTAB, a swelling agent (n-octane), and a base catalyst (NH4OH). In order to enhance DOX cellular uptake as well as minimize self-aggregation, the outermost surfaces of MSNs were functionalized with trimethylammonium (TA) groups that could enhance the NP's surface charge. At higher positive charges of the surface of TA-modified MSNs, higher rate of the cellular internalization was observed. Therefore, surface charge modulation of MSNs through the decoration of positively charged TA groups could be directly associated with cellular uptake and cytotoxicity potential (Lee et al., 2010).

In a study, pentamidine, as an antiprotozoal agent, was loaded into bare and functionalized MSNs including carboxypropyl-, aminopropyl- and cyanopropyl-MSNs to compare the drug release profile. This study revealed that aminopropyl-MSNs had positive ζ potential values, carboxypropyl-MSNs had negative ζ potential values, while the cyanopropyl-MSNs were neutral. Based on the results, only the negatively-charged MSNs including MSN-OH and MSN-COOH, were effective while the neutral or positively-charged MSNs (MSN-CN and MSN-NH$_2$) were not. These results can be attributed to a proton transfer from Si-OH and -COOH surface group to pentamidine that can lead to the formation of a complex that is stabilized by electrostatic interactions. In contrast, the positively-charged MSN-NH$_2$ in the aqueous medium and the neutral environment correspond to the MSN-CN could not result in a stable drug loading. Furthermore, faster pentamidine release from MSN-OH was observed, while pentamidine was released more gradually from MSN-COOH. The obtained results showed the effect of hydrophobic interactions between the drug molecule and the propyl graft chains of MSN-COOH on drug encapsulation and stabilization inside the MSNs' pores that can lead to a sustained release pattern (Peretti et al., 2018).

In order to provide mixed-charged brush MSNs, the surface was modified with two silane molecules (-NH$_3^+$/−PO$_3^-$), and their low-fouling capability, surface characteristics, and cellular uptake were compared with PEGylated MSNs. The MSN functionalization process consisted of the simultaneous direct-grafting of the hydrolyzable short-chain amino (aminopropyl silanetriol) and phosphonate-based (trihydroxy-silyl-propyl-methyl-phosphonate) silane molecules to induce a pseudo-zwitterionic nature at physiological pH states. The results showed that both mixed-charged pseudo-zwitterionic MSNs and PEG-MSN induced a significant reduction in serum protein adhesion and cellular uptake regarding to pristine MSNs. Regarding pseudo-zwitterionic MSNs, this reduction was up to 70%–90% for protein adsorption and up to 60% for cellular uptake. Pseudo-zwitterionic MSNs could enhance targeted local drug delivery by the synergistic effect of the capability of the nanocarriers to deliver active pharmaceuticals to the specific site and also the induce of electrostatic interactions between the mixed-charge MSNs and bacteria (Encinas et al., 2019).

Briefly, MSNs with higher surface charge could enhance cellular uptake. Higher particle charges (regardless of positive or negative charges) result in higher cellular uptake in comparison to the neutral

net charge. However, the positive net charge would be superior to the negative charge for the purpose of cellular uptake enhancement. In addition, MSNs with positive surface area show higher dissolution rates and improve the biological effects. Moreover, the electrostatic attraction between the loaded drug and the MSNs surface charge can lead to a sustained drug release profile.

3 Organ-based toxicity of MSNs

3.1 Nephrotoxicity of MSNs

After entering the bloodstream MSNs can as well enter the lymph and thus access various organs and tissues (Sarkar et al., 2014). The kidney as one of the main excretory organs, is supplied with large amounts of blood vessels. In this regard, MSN-induced renal toxicity should be considered (Chen et al., 2015). MSNs that circulate in the blood can be filtered by the kidney and by means of the glomerular filtration barrier. Glomerular endothelial cells and glomerular basement membrane and podocytes are components of the glomerular filtration barrier (Kamaly et al., 2016; George et al., 2017).

A number of *in vitro* and *in vivo* reports showed the potential toxicity of MSNs (Murugadoss et al., 2017). Although the nephrotoxicity of MSNs has been mentioned in these studies, the mechanism of renal toxicity caused by MSNs is still not fully elucidated (Mahmoud et al., 2019a). MSNs can induce oxidative stress, inflammation, fibrosis, autophagy, and at last organ injury (Chou et al., 2017; Zhang et al., 2018b; Hozayen et al., 2019).

3.1.1 Mechanisms involved in nephrotoxicity of MSNs

3.1.1.1 Activation of TLR4/MyD88/NF-κB signaling pathway

The mechanism of nephrotoxicity of MSNs is probably through inflammation and oxidative stress, which is governed through the activation of the nuclear factor-kappa B (NF-κB) pathway (Xi et al., 2016; Mahmoud et al., 2019a) (Chen et al., 2015). NF-κB is considered as a transcription factor for regulating inflammation (Yuan et al., 2020). NF-κB contributes markedly to various cellular functions from cell survival to cell death, as well as predisposition to various diseases. Regulation of the immune system, inflammation, function of the nervous system as well as the development of cancer are influenced by the signaling of NF-κB (Yamamoto and Gaynor, 2001; Mahmoud et al., 2019a). Toll-like receptors (TLRs) can be considered as an important class of protein molecules that are involved in non-specific immunity and can act as a bridge between non-specific and specific immunity. TLRs are a family of transmembrane receptors that can activate downstream proinflammatory cascades. In fact, innate immune cells detect danger signals through TLR engagement. One of the downstream pathways of TLR4 is TLR4/MyD88/NF-κB signaling pathway, which ultimately leads to NF-κB activation and inflammation (Zhang et al., 2022). Activation of NF-κB can increase the expression and release of pro-inflammatory cytokines such as tumor necrosis factor alpha (TNF-α) and interleukin-6 (IL-6) and can also cause the accumulation of infiltrating inflammatory cells in the kidney. In conclusion, all of these can lead to inflammation in the kidney (Hu et al., 2020; Ren et al., 2020). Inflammation that is caused by the

production of pro-inflammatory cytokines, can eventually lead to damage to the nephrons and kidneys (Chen et al., 2018) and may often lead to chronic kidney disease (CKD) (Qian, 2017). MSNs can increase the release of TNF-α, interleukin-1 beta (IL-1β), and IL-6 by activating NF-κB. In general, NF-κB plays an important role in inflammation and oxidative stress, and studies have shown that silica nanoparticles can activate NF-κB (Waters et al., 2009; Chen et al., 2015). Toll-like receptor 4 (TLR4) activation and Myeloid differentiation primary response 88 (MyD88) play an effective role in NF-κB activation (Winkler et al., 2017). It has been observed that the expression of TLR4 and MyD88 was increased in MSN-receiving rats. Therefore, the TLR4/MyD88/NF-κB signaling pathway may be involved in the kidney damage caused by MSNs (Mahmoud et al., 2019a).

3.1.1.2 Oxidative stress and overproduction of reactive oxygen species (ROS)

The main mechanism involved in MSN-induced nephrotoxicity is oxidative stress. As ROS production increases, an imbalance is created between the ROS level and the antioxidant defense, which ultimately leads to oxidative stress (Chen et al., 2008; Hayyan et al., 2016). Increased levels of ROS disrupt the natural mechanism of cell metabolism, which can eventually lead to inflammation and DNA damage, cell cycle arrest, and ultimately cell apoptosis (Nemmar et al., 2016; Xiao et al., 2016; Reddy et al., 2017). Apoptosis in renal tubular epithelial could be of the main cause of tubular dysfunction (Basile et al., 2012; Berger and Moeller, 2014). ROS can also cause podocyte injury or reduce podocyte activity (Xu et al., 2012) (Xu et al., 2013) (Wolf et al., 2005). It has been shown that different types of MSNs can induce the production of intracellular ROS. However, NP size, chemical composition, and surface reactivity contribute substantially in this regard (Møller et al., 2010; Thit et al., 2015; Xiao et al., 2016; Reshma and Mohanan, 2017).

MSNs can increase ROS in kidneys in a dose-dependent manner. Overproduction of ROS can lead to lipid peroxidation and induce damage to cellular proteins and DNA (Sun et al., 2011; Zuo et al., 2016). In MSNs-administered rats, it has been observed that following excessive production of ROS, there is an increase in malondialdehyde level, and a reduction in glutathione level, superoxide dismutase, catalase (CAT), and glutathione peroxidase activity. These findings refer to the state of oxidative stress caused by MSN in the kidneys of rats (Yu et al., 2017a).

MSNs can also increase nitric oxide (NO) production in rat kidneys. The increase in the expression of inducible NO synthase (iNOS) can lead to the overproduction of ROS and ultimately the synthesis of pro-inflammatory cytokines (Xue et al., 2014; Mahmoud et al., 2019a).

In the studies conducted on MSNs, it has been determined that they have the ability to produce intrinsic ROS and can activate nicotinamide adenine dinucleotide phosphate (NADPH) oxidase [NOX] and cause mitochondrial dysfunction (Fubini and Hubbard, 2003; Chen et al., 2015). The redox potential sensor transient receptor potential melastatin 2 (TRPM2) is responsible for the regulation of NOX activity and ROS generation in the human embryonic kidney 293 cell line (HEK293) treated with MSNs (Chen et al., 2015).

3.1.1.3 Suppression of Nrf2/ARE/HO-1 signaling pathway

Nuclear factor erythroid 2-related factor 2 (Nrf2) is a transcription factor that can regulate the expression of antioxidants such as heme oxygenase (HO-1) (Satta et al., 2017). The main function of Nrf2 is the activation of the antioxidant response. If mild oxidative stress is present, ROS can disrupt the Keap1–Cullin 3 ubiquitination system, which degrades Nrf2. Therefore, Nrf2 can translocate into the nucleus and form a complex with small MAF and bind to the antioxidant response element (ARE), which ultimately can increase the expression of antioxidant genes (Itoh et al., 1997) (Villeneuve et al., 2010). In general, the activation of Nrf2 signaling can lead to an increase in antioxidants and a decrease in ROS levels. It has been found that MSN-administered rats can possibly inhibit Nrf2 in a dose-dependent manner. Also, a decrease in HO-1 expression along with a decrease in antioxidant enzymes has been observed in MSN-administered rats. These could indicate override and sustained oxidative stress in MSN-receiving rats (Mahmoud et al., 2018; ALHaithloul et al., 2019; Mahmoud et al., 2019a; Mahmoud et al., 2019b).

3.1.1.4 Activation of JAK2/STAT3 signaling pathway

MSNs may also activate the Janus kinase 2/signal transducer and activator of the transcription 3 (JAK2/STAT3) signaling pathway. STAT3 may be involved in MSN-induced fibrosis since MSNs can increase the phosphorylation of JAK2 and STAT3 in rat kidneys (Levy and Darnell, 2002; Ogata et al., 2006; Mahmoud et al., 2019a). MSNs may also promote fibrosis induced by the enhanced collagen expression (Mahmoud et al., 2019a).

3.1.2 Laboratory studies
3.1.2.1 In vivo studies

In a study on MSN-administered rats, increased renal toxicity with a significant elevation in serum creatinine and urea was observed. Serum creatinine increased on day 14 after intragastric administration of 40 mg/kg MSNs in rats. Following consumption of 25 mg/kg MSNs, various kidney damages including tubular degeneration, glomerulonephritis, glomerular hypercellularity, chronic nephritis, and leukocyte infiltration were reported. At the dose of 50 mg/kg of MSNs, tubular necrosis was observed as well. In higher doses, glomerular atrophy, casts, tubular dilatation, cystic, and Bowman's capsule dilatation occurred. Following the injection of 300 and 600 mg/kg MSN, on day 12, lymphocytic infiltration, interstitial fibrosis, and renal tubular regeneration were observed in mice. As a result, MSNs can affect the function and structure of kidneys (Mahmoud et al., 2019a).

In another study, it has been determined that IP administration of MSNs in mice has the ability to cause selective acute kidney toxicity in the early stages, which can lead to interstitial fibrosis of renal tubules. In this study, inflammation has been introduced as the main cause of acute kidney toxicity induced by MSNs, which is modulated by the NF-κB signaling pathway (Chen et al., 2015).

The toxicity of MSNs after a single IP administration also has been investigated in BALB/c mice. Severe spread of renal interstitial inflammatory reactions and hyperemia of renal tubules were identified in the histological studies. Also, the increase in BUN and serum creatinine levels, which are very sensitive indicators of

kidney toxicity, indicate MSN-induced kidney function injury (Wang et al., 2022).

3.1.2.2 *In vitro* studies

In vitro studies can sometimes be controversial in the global framework of nano-toxicity. Controversial results in such studies may be due to differences in production processes or life cycles of NPs or dispersion methods, which ultimately lead to differences in surface characteristics and reactivity of NPs. Therefore, precise control of the physical and chemical properties of the tested NPs is essential (Barillet et al., 2010).

In order to investigate renal toxicity of NPs, different cell lines are used among which glomerular mesangial cells (IP15) (L'azou et al., 2008), epithelial proximal tubular cells (LLC-PK1, NRK-52E, HK-2) (Passagne et al., 2012) (Valentini et al., 2017), epithelial distal tubular cells (MDCK) (Yamagishi et al., 2013), HEK293 (Wang et al., 2009), porcine kidney (PK 15) (Milić et al., 2015) are mostly used however, depending on the type of the cell line toxicity result may vary.

In an *in vitro* study conducted on rat kidney cell line (NRK-52E), cytotoxicity and fibrosis markers, and NF-κB pathways were investigated. It was determined that MSNs can cause cytotoxicity and can increase the expression of fibrosis markers and can induce NF-κB pathway activation (Chen et al., 2015).

In a study, the genotoxicity of MSNs in HEK293 cells has been investigated. For this purpose, HEK293 cells were treated with 100 μg/mL MSNs for 24 h. As a result, it has been found that MSNs can significantly alter the expression of various genes. MSNs have been able to cause upregulation in the expression of 579 genes and downregulation in the expression of 1263 genes. This genotoxicity may induce cellular dysfunction and other benign diseases (Zhang et al., 2015).

3.1.3 Proposed solutions to reduce MSNs nephrotoxicity

forkhead box protein O3 (FOXO3) belongs to the O subgroup of the forkhead family of transcription factors. FOXO3 can act as a regulating factor in various cell functions including growth, metabolism, and survival (Nho and Hergert, 2014). FOXO3 can also regulate oxidative stress and inflammatory process. FOXO3 can promote the gene transcription of MnSOD and CAT by binding to the gene promoter region and ultimately increase the level of ROS (Shi et al., 2019a; Han et al., 2020). FOXO3 can also bind to NF-κB and eventually lead to the inhibition of NF-κB activity (Hwang et al., 2011). Therefore, in general, upregulation of FOXO3 activity may be able to delay the inflammatory process and increase the antioxidant capacity of the cell. This can make FOXO3 a therapeutic target for MSN-induced nephrotoxicity (Wang et al., 2022). Apigenin, which is a phytochemical flavonoid, can be effective in the regulation of FOXO3 levels. Apigenin can inhibit NF-κB activity and thus lead to a reduction in the level of pro-inflammatory cytokines (Sun et al., 2016; Ranucci et al., 2020). Therefore, Apigenin may prevent MSN-induced renal cytotoxicity by reducing inflammation and oxidative stress (Wang et al., 2022). In a study, the effect of Apigenin on MSN-induced nephrotoxicity has been investigated. It has been found that Apigenin can decrease the level of BUN and serum creatinine and increase

the level of superoxide dismutase, glutathione, and CAT and improve the pathological changes caused by MSNs in the kidneys of mice (Wang et al., 2022).

The potential effects of the route of administration, particle size, and dose on the nephrotoxicity of MSNs are summarized in Table 1.

3.2 Hepatotoxicity of MSNs

Numerous studies have reported that several factors including particle size, porosity, animal sex, and duration of exposure can affect the hepatotoxicity of MSNs (Mohammadpour et al., 2019).

3.2.1 Mechanisms involved in the hepatotoxicity of MSNs

The liver is a specific immunological and anatomical site in which blood is perfused through a network of sinusoids. Different zones of the liver are responsible for different functions. Blood antigens in the liver can be scanned by antigen-presenting cells and lymphocytes. The liver as a multicellular structure has four lobes which are subdivided into hexagonal-shaped lobules (Racanelli and Rehermann, 2006; Thompson and Takebe, 2021). The liver is a major organ for immune defense and metabolism. Studies have elucidated that many nanoparticles prefer to accumulate in the liver. Although they can participate in the treatment of liver diseases such as liver fibrosis, viral hepatitis, and liver cell carcinoma, however, they can also cause liver injury. Their hepatotoxicity effects depend on the size, charge, dose, and modification of the MSNs. An increasing number of studies have found that nanomaterials can trigger the immune system and elevate ROS levels, leading to liver damage. Kupffer cells (KCs) as specialized macrophages have an important role in the clearance of substances such as MSNs, gut-derived bacteria, and bacterial toxins. Autophagy is a critical dynamic intracellular process for cell hemostasis and often has a protective role in the liver. Impaired autophagy in KCs exacerbates liver injury in diseases like liver fibrosis, toxin-induced liver injury, and alcoholic liver disease (Zhu et al., 2017).

Herein, we provide an overview of different molecular mechanisms involved in the hepatotoxicity of MSNs as well as available data on their liver toxicity in cell cultures, animal models, and at last, present data from available clinical studies. A schematic view of the main pathways involved in the hepatotoxicity and nephrotoxicity of MSNs is depicted in Figure 1.

MSN can induce oxidative stress, inflammation, fibrosis, and liver injury. Activation of TLR4/MyD88/NF-κB and JAK2/STAT3 signaling, suppression of the Nrf2/ARE/HO-1 pathway, pyroptosis, and autophagy are involved in MSN hepatotoxicity (Mahmoud et al., 2019a) and are discussed in the upcoming sections.

3.2.1.1 Activation of TLR4/MyD88/NF-κB signaling pathway

Silica nanoparticles can activate NF-κB and accordingly increase the release of TNF-α, IL-1β, and IL-6. NF-kB is a group of inducible transcription factors that protect cells from cellular stress and pyroptosis. As was mentioned in the literature review the expression of TLR4 and MyD88 increases in MSN-administered rats. Different cells such as Kupffer cells, hepatocytes, and hepatic

TABLE 1 The effect of route of administration, particle size, and dose on the nephrotoxicity of MSNs.

Nanoparticles	Type of study	Route of administration	Particle size	Dose	Exposure time	Result	Ref.
MSNs	Animal study (Balb/c mice)	single intraperitoneal injection	-Round with a homogeneous pore structure inside −198.2 ± 21.8 nm	150, 300, or 600 mg/kg	2 and 12 days	-Renal interstitial fibrosis -Regeneration of renal tubules -Increase the expression of fibrosis markers and the nuclear translocation of NF-κB p65 in the kidney sample -Induce AKI at the preliminary stage -Development of renal tubular-interstitial fibrosis -Inflammation is a major initiator of the AKI induced by MSNs, that is mediated by the NF-κB signaling pathway	Chen et al. (2015)
MSNs	Cell line (NRK-52E)		-Round with a homogeneous pore structure inside −198.2 ± 21.8 nm	25, 50, 100, 200, 400, 800, 1000 (µg/mL)	3 and 24 h	-A dose- and time-dependent NRK-52E cell viability reduction -Cytotoxicity in NRK-52E cells and enhanced the expression of fibrosis markers.	Chen et al. (2015)
MSNs	Animal study (Balb/c mice)	single intraperitoneal injection	-Uniform and roughly spherical in shape −203.2 ± 17.5 nm	300 mg/kg	7 days	-Renal interstitial inflammatory reactions cell infiltration, and hyperemia of renal tubules -Increased BUN and serum creatinine	Wang et al. (2022)
MSNs	Cell line (NRK-52E)		-Uniform and roughly spherical in shape −203.2 ± 17.5 nm	400 µg/mL	24 h	-Decrease cell viability	Wang et al. (2022)
MSNs	Animal study (Wistar rats)	single intraperitoneal injection	-Spherical, non-aggregated, well-dispersed particles - 50 nm	25, 50, 100 and 200 mg/kg	30 days	-Increase BUN and serum creatinine -Tubular degeneration, glomerulonephritis, glomerular hypercellularity, chronic nephritis, and leukocyte infiltration -Tubular necrosis, tubular dilatation, Bowman's capsule dilatation, glomerular atrophy, casts, and cystic fibrosis	Mahmoud et al. (2019a)
MSNs	Cell line (HEK293)		100 nm	100 µg/mL	24 h	-Upregulation of 579 genes expression -Downregulation of 1263 genes expression	Zhang et al. (2015)

stellate cells widely express TLRs. TLR-mediated signaling is involved in liver injury. MSN suppresses Nrf2 and Nrf2 suppression can be involved in the activation of NF-kB signaling. In conclusion, the loss of Nrf2 function exhibits oxidative stress and exacerbates inflammation. Furthermore, overexpression of the NF-kB p65 subunit can increase nuclear keap 1 and inhibit Nrf2 signaling but the effect of keap 1 on the deactivation of Nrf2 within the nucleus has not yet been definitively stated and is under discussion. Nrf2 is an upstream regulator of proinflammatory cytokine production (Mahmoud et al., 2019a).

3.2.1.2 Activation of JAK2/STAT3 signaling pathway

Janus protein tyrosine kinase (JAK2) can activate signal transducer and activator of transcription (STAT3). Activation of STAT3 may be involved in MSN-associated fibrosis. Promotion of JAK2 and STAT3 phosphorylation occurs by MSNs. Persistent activation of STAT3 is accompanied by different pathological states such as fibrosis. The exact molecular mechanisms of STAT3 in fibrosis are still remained to be clear but some studies have demonstrated that STAT3 triggers the production of collagen type 1 (Mahmoud et al., 2019a; Zhao et al., 2021). The collagen
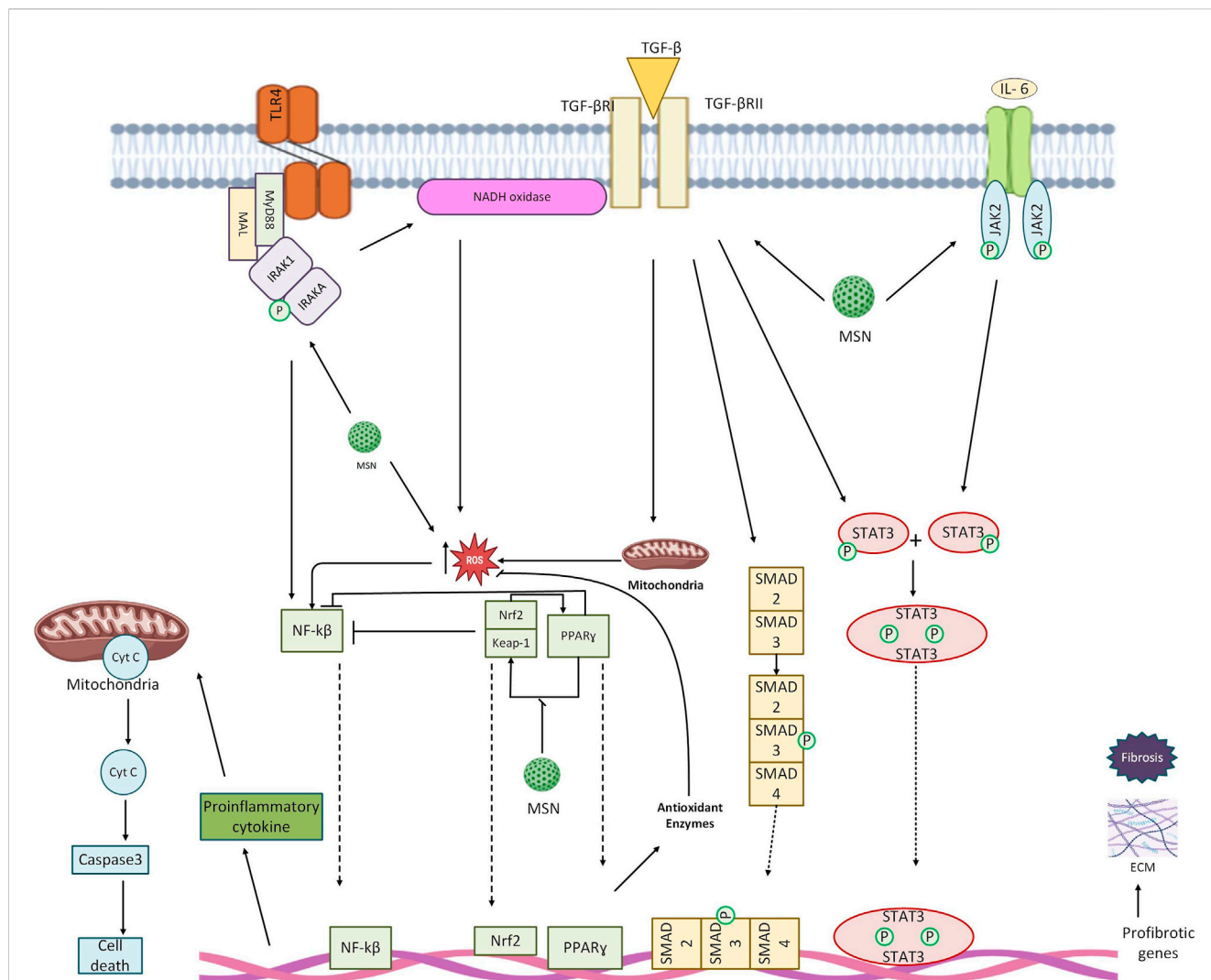
FIGURE 1
Activation of TLR4/MyD88/NF-κB signaling pathway, induction of oxidative stress and overproduction of ROS, activation of JAK2/STAT3 signaling pathway, upregulation of proinflammatory cytokines, induction of apoptosis, overexpression of PPARγ all may lead to hepatotoxicity and nephrotoxicity of MSNs.

family is an extracellular matrix protein that is used to provide structural support to connective tissue and form the basement membrane of the liver. Different types of collagens exist. Various types of collagen such as type I, III, and V are mostly involved in liver fibrosis. Elevation in the expression of type I collagen is considered as the most characterized aspect of liver fibrosis (Tsukada et al., 2006).

3.2.1.3 Suppression of Nrf2/ARE/HO-1 signaling pathway

Nrf2/ARE/HO-1 signaling pathway is involved in ROS production which ultimately leads to the destruction of hepatocytes. Nrf2 as a transcription factor govern the expression of HO-1 as an antioxidant. In pathological conditions, extra- and intra-cellular levels of free heme probably increased because of the release from hemoproteins. Free heme has pro-inflammatory and oxidative properties and can act as a dangerous signal. HO which degrades heme with

antioxidants effects has two isoforms. Inducible HO-1 and constitutively expressed HO-2. ROS degrades Nrf2 through the disturbance of the keap1-cullin3 ubiquitination system. Increased expression of antioxidant genes occurs after translocation of Nrf2 into the nucleus, complex with small MAF, and binding to antioxidant response element (Lundvig et al., 2012; Mahmoud et al., 2019a). In conclusion, as Nrf2 is inactivated antioxidant properties decline and ROS levels increase. A recent study on MSN-administered rats has demonstrated that Nrf2 suppression can lead to liver fibrosis in a dose-dependent manner.

3.2.1.4 Apoptosis

Persistent apoptosis is the main factor involved in MSN-associated liver fibrosis. Membrane blebbing, chromatin condensation, cell shrinking, inter-nucleosomal DNA fragmentation, and the formation of small vehicles occur in

apoptosis. Caspases mediate all biochemical and morphological changes related to apoptosis. The death receptor pathway is an extrinsic pathway that mediates death signaling by the superfamily of death receptor transmembrane proteins. Trimerization and clustering of receptors happen as ligands bind to the receptors to recruit adapt protein such as Fas-associated via the death domain and facilitate their binding to procaspase 8. Caspase 3 is activated after auto-catalyzation and activation of caspase 8. This pathway leads to initiation of the execution phase of apoptosis. Different types of oxidative stress such as DNA damage, hypoxia, growth-factor deprivation, and mitochondrial membrane permeabilization initiate the intrinsic pathway of apoptosis. Dimerization and insertion of proapoptotic proteins including BAX and BAK1 into the outer mitochondrial membrane trigger the intrinsic pathway of apoptosis. Cytochrome C is released into the cytosol through permeabilized mitochondria, binds to apoptotic peptidase activating factor1 (APAF1), and starts the formation of apoptosomes. Apoptosomes have a substantial role in the recruitment and activation of CASP9, CASP3, CASP6, and CASP7 which further leads to apoptosis. After apoptosis, KC rapidly engulf apoptotic hepatocytes and the accumulation of apoptotic bodies induces the production of TNF-α and the release of TGF-B1 (Mahmoud et al., 2019a; Mohammadinejad et al., 2019).

3.2.1.5 Peroxisome proliferator-activated receptor gamma (PPARγ)

Peroxisome proliferator-activated receptor gamma (PPARγ) significantly protects the liver from oxidation, inflammation, fibrosis, fatty liver, and tumor formation. Activation of the expression of antioxidant enzymes, NF-κB and TGF-β1/Smad3 suppression occurs by PPARγ (Mahmoud et al., 2019a; Wu et al., 2020). A previous study has shown that MSNs distribute in the hepatocytes, KC, hepatic stellate cells (HSC), and fibroblast cells leading to activation of the TGF-β1/Smad3 signaling pathway and liver fibrosis (Yu et al., 2017b). Additionally, overexpression of PPARγ has been shown to cause remarkable liver fibrosis, suppressed HSC, and fibrogenesis in PPARγ-deficient mice. PPARγ downregulate in MSN-treated mice (Mahmoud et al., 2019a).

3.2.1.6 Pyroptosis

Pyroptosis is a novel caspase-1-dependant form of programmed cell death which is characterized by forming pores on the plasma membrane, swelling cells, and disrupting the plasma membrane with a large number of pro-inflammatory factors. Nucleotide-binding oligomerization domain-like receptor protein 1 (NLRP1) and nucleotide-binding oligomerization domain-like receptor protein 3 (NLRP3) as pattern recognition receptors (PRR) bind to pro-caspase-1 and change it into mature caspase-1. It can also release IL-1β and interleukin-18 (IL-18) that can induce inflammatory responses. Inflammasomes as polyprotein complexes distinguish damage- and/or pathogen-related molecular patterns and induce pyroptosis. A recent in vitro study has demonstrated that MSN hepatotoxicity may be due to inducing NLRP3 in a dose and time-dependent manner (Zhang et al., 2018b; Zhang et al., 2021).

3.2.1.7 Autophagy

Autophagy or self-eating is an emerging process that degrades misfolded protein and dysfunctional organelles in lysosomes. As mentioned earlier, a recent study has demonstrated that MSN induces toxicity through activation of the NF-kB pathway and release of IL-1β and TNF-α. MSNs upregulate the levels of Beclin-1 and LC3II as markers of autophagy in MSN-treated cells. It is worth noting that autophagy enhances inflammation mediated by the NF-kB pathway. In conclusion, different studies suggested that autophagy can be a possible protective factor in inflammation caused by MSN in macrophages (Xi et al., 2016; Li and Ju, 2018).

3.2.2 Laboratory studies
3.2.2.1 In vivo studies

Several in vivo studies have been carried out on different breeds of mice to evaluate the hepatotoxicity of MSNs. Studies that administered MSNs via the IV route have shown that ROS generation, liver inflammation, hepatic cell pyroptosis, and as a result hepatotoxicity was induced (Zhang et al., 2018b; Li et al., 2022). The increasing levels of aspartate aminotransferase (AST)/alanine aminotransferase (ALT) and the inflammatory factors IL-6, IL-1β, and TNFα as well as glutathione peroxidase, superoxide dismutase 3, Glucose-6-phosphate dehydrogenase (G6PD), hexokinase (HK), and phosphofructokinase (PFK) at proteomic and transcriptomic levels were increased. On the other hand, oxidative phosphorylation, tricarboxylic acid (TCA), and mitochondrial energy metabolism were decreased (Li et al., 2022). Another study has indicated that an increase in particle size elevates MSN hepatotoxicity (Mohammadpour et al., 2019).

IP administration of MSNs is suggestive of a rise in liver injury markers such as ALT, IL-1 β, TNF-α, lymphocytic infiltration, silicotic nodular-like lesions, and collagen fibers as well as a dramatic incline in hydroxyproline. Levels of ROS, lipid peroxidation, and NO are shown to be elevated as well. On the contrary, suppression of the Nrf2/HO-1 signaling pathway along with antioxidant capacity have been documented. Other observed mechanisms embracing MSN hepatotoxicity, are regulation of the expression of TLR4, MyD88, NF-κBp65, and caspase-3. MSNs also activate the JAK2/STAT3 signaling pathway and downregulate PPARγ and promote liver fibrosis (Liu et al., 2012; Mahmoud et al., 2019a). A study has shown that liver and spleen weight increase significantly and lymphocyte population changes in the spleen following MSN administration (Lee et al., 2013).

Oral administration of MSNs has been shown to disturb inflammatory factors and metabolites of ribose-5-phosphate, 6-phosphogluconate, Glutathione disulfide (GSSG), as well as nicotinamide adenine dinucleotide phosphate (NADP+) associated with the pentose phosphate pathway, glutathione synthesis, and oxidative stress (Li et al., 2022). Another study has indicated that short-term oral administration of non-porous silica nanoparticles and MSNs was not associated with systemic or local toxicity in mice (Cabellos et al., 2020).

3.2.2.2 In vitro studies

An in vitro study has shown that MSNs cause liver inflammation, hepatic cell pyroptosis, hepatotoxicity, and increase ROS generation (Zhang et al., 2018b).

TABLE 2 The effect of route of administration, particle size, and dose on the hepatotoxicity of MSNs.

Nanoparticles	Type of study	Route of administration	Particle size	Dose	Exposure time	Result	Ref.
MSN	Cell line (L02 cells)	-	109.2 nm	-	24 and 48 h.	-Liver inflammation, hepatotoxicity, and hepatic cell pyroptosis	Zhang et al. (2018b)
						-Increase ROS generation	
MSN	Animal study (BALB/C mice)	Intravenous injection	109.2 nm	50 mg/kg	Three times a week for 3 weeks	-Liver inflammation, hepatotoxicity, and hepatic cell pyroptosis, and -Increase ROS generation	Zhang et al. (2018b)
MSN	Animal study (BALB/C mice)	Intraperitoneal injection	~100 nm	2,20 and 50 mg/kg/day	5 days/week for 4 weeks	-Increase significantly in liver and spleen weight.	Lee et al. (2013)
						-Lymphocyte population change in the spleen.	
MSN	Animal study (Female ICR mice)	Intraperitoneal injection	~110 nm	10,25 and 50 mg/kg	Twice a week for 6 weeks	-Increase liver injury markers including alanine aminotransferase (ALT) and inflammatory cytokines including IL-1β and tumor necrosis factor-alpha (TNF-α)	Liu et al. (2012)
						-Lymphocytic infiltration, silicotic nodular-like lesions, and Collagen fibers have been observed.	
						-Increase dramatically hydroxyproline level	
MSN	Animal study (male Wister Rats)	Intraperitoneal injection	~50 nm	25,50,100, and 200 mg/kg	30 days	-Increase ROS, nitric oxide production, and lipid peroxidation	Mahmoud et al. (2019a)
						-Suppress antioxidants and Nrf2/HO-1 signaling in the kidney and liver.	
						-Regulate expression of TLR4, MyD88, NF-κBp65, and caspase-3.	
						-Increase serum pro-inflammatory cytokines.	
						-Activate the JAK2/STAT3 signaling pathway	
						-Down-regulate the peroxisome proliferator-activated receptor gamma (PPARγ) and promote fibrosis.	

TABLE 2 (*Continued*) The effect of route of administration, particle size, and dose on the hepatotoxicity of MSNs.

Nanoparticles	Type of study	Route of administration	Particle size	Dose	Exposure time	Result	Ref.
MSN	Animal study (male ICR mice)	-Intravenous -Oral administration	~80 nm	- 20 mg/kg/d - 200 mg/kg/d)	10 days	**IV injection:** -Induce inflammation -Increase the levels of AST/ALT and the inflammatory factors including IL-6, IL-1β, and TNF-a -Increase in glutathione peroxidase, superoxide dismutase 3, HK, G6PD, and PFK at proteomic and transcriptomic levels -Reduce oxidative phosphorylation, TCA, and mitochondrial energy metabolism **Oral administration:** -Disturb inflammatory factors and metabolites of GSSG, ribose-5-phosphate, 6-phosphogluconate, and NADP + associated with the pentose phosphate pathway, oxidative stress, and glutathione synthesis	Li et al. (2022)
MSN	Animal study (male ICR mice)	Intragastrical injection	85 nm	40 mg/kg	Single dose	-MSN has shown decreasing *in vivo* biodegradation, absorption, and excretion, decrease liver distribution and urinary excretion as the aspect ratio increase.	Li et al. (2015a)
MSN	Animal study (female Swiss mice)	Oral gavage	100 and 300 nm	100 and 1000 mg/kg b.w.	5 consecutive days	-No systemic or local toxicity after short-term oral administration.	Cabellos et al. (2020)
MSN	Animal study (Male albino B6 mice)	Intravenous, subcutaneous, and Intraperitoneal injection	200 nm	250–2000, 23–260, or 1–71 mg/kg of HMS particles	Single dose	-The lowest lethal dose toxicity, the maximum tolerated dose, and allergy-inducing ability in HMS are the same in MSN. -Lower inflammation has been shown in HMS	Sun et al. (2021)
MSN	Animal study (BALB/C mice)	Intravenous administration	50 and 500 nm	40–700 mg/kg	10–60–180 days	-Increasing particle size elevates toxicity. -SNPs accumulation in the liver would be time-dependent -Cytokine levels increased dramatically on day 60	Mohammadpour et al. (2019)

(Continued on following page)

**TABLE 2 (*Continued*) The effect of route of administration, particle size, and dose on the hepatotoxicity of MSNs.**

Nanoparticles	Type of study	Route of administration	Particle size	Dose	Exposure time	Result	Ref.
MSN	Animal study (female and male BALB/c mice)	Intravenous administration	432.0 ± 18.7 nm, 46 ± 4.9 nm, and 466.0 ± 86.0	100 mg kg−1 in females and 40 mg kg−1 in male	Single dose	-Microscopic lesions in the liver, spleen, kidney, or lung has found. -Pathological lesions were found in animals injected by large, nonporous SNPs.	Mohammadpour et al. (2020)
MSN	Animal study (female BALB/c mice)	Intraperitoneal injection	~150 nm	150, 300 of 600 mg/kg MSN	Single dose	-Potential protective roles of autophagy against a large dose of MSN have been shown in this study.	Xi et al. (2016)
MSN	Animal study (Male ICR mice)	Intravenous injection	64.43 ± 10.50 nm	20 mg/kg	Every 3 days for 5 times	-Silica nanoparticles can cause liver fibrosis by inducing oxidative stress and apoptosis.	Yu et al. (2017b)

The bold letters were used to distinguish the results of the oral and IV routes of administration.
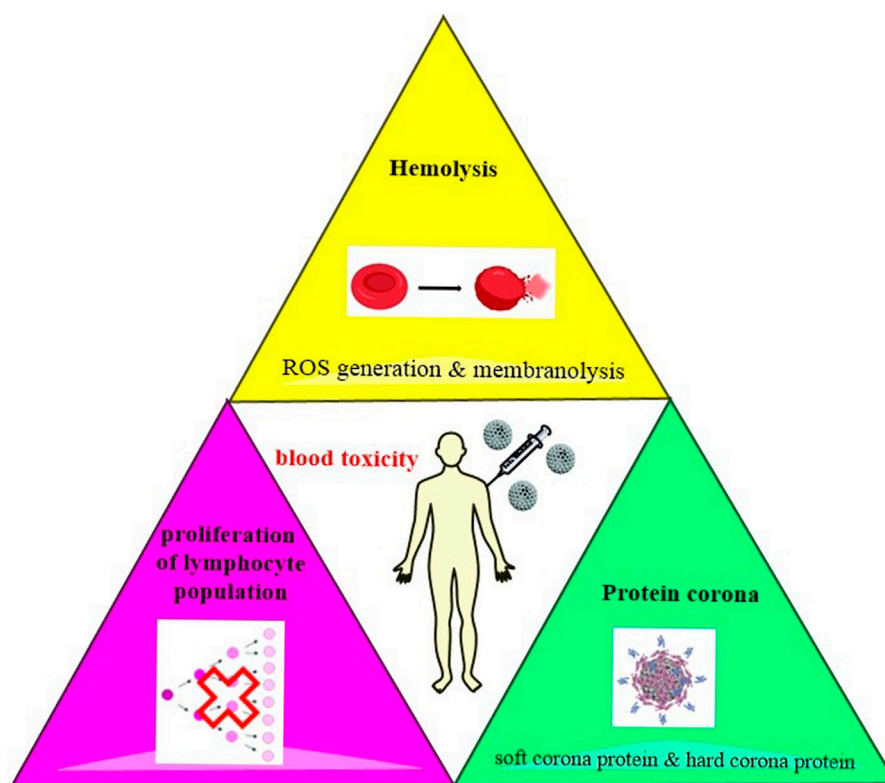
FIGURE 2
Induction of hemolysis which happens mainly by the production of ROS, the proliferation of lymphocyte population, and formation of protein cornea are among the main mechanisms involved in the hematotoxicity of MSNs.

3.2.3 Proposed solutions to reduce MSNs hepatotoxicity

Size and surface modification of MSNs can be used to avoid the side effect of MSNs (Zhang et al., 2018b). A study conducted on ICR mice treated by spherical MSNs has shown that MSNs and PEGylated MSNs with different ranges of sizes distribute mainly in the liver and spleen. Smaller and PEGylated MSNs escape more easily from liver capturing (He et al., 2011). MSN shapes are another factor that can be a solution to reduce their adverse effects. A study has indicated that short-rod MSNs are more

readily accumulated in the liver than long-rod MSNs (Wani et al., 2017).

The potential effects of the route of administration, particle size, and dose on the hepatotoxicity of MSNs are summarized in Table 2.

3.3 Blood toxicity of MSNs

Blood can be considered as a gateway that delivers all NPs to the target tissue or organ (Matus et al., 2018). Therefore, the interaction of NPs with blood components is inevitable and hemocompatibility should be considered in the design and development of therapeutic NPs (de la Harpe et al., 2019). One of the methods usually used to evaluate the hemocompatibility of MSNs is the hemolysis assays, however, it is important to note that hemolysis assays cannot separately indicate the compatibility of NPs with erythrocytes (Yu et al., 2011; Krajewski et al., 2013). Optical analysis and deformability assessments can provide a better over view of the effect of NPs on red blood cells (RBCs) (de la Harpe et al., 2019).

3.3.1 Mechanisms involved in blood toxicity of MSNs

RBCs, white blood cells (WBCs), and platelets are the main cellular components of the blood and each of these blood cells has a unique structure and function (Scanlon and Sanders, 2018). Plasma proteins can rapidly attach to the surface of NPs and create a protein corona that can effectively interact NPs with blood components (Ritz et al., 2015). A schematic view of molecular mechanisms involved in the blood toxicity of MSNs is shown in Figure 2.

3.3.1.1 Hemolysis

MSNs induce hemolysis that can occur by two mechanisms including ROS generation that can induce cell death through apoptosis or necrosis and membranolysis caused by electrostatic interactions between MSNs and tetra-alkyl-ammonium-containing phospholipids. Silica consists of terminal silanol groups. Hemolysis occurs less in MSNs than in nonporous silica NPs due to the accessibility of the surface silanols (Morrow and McFarlan, 1992; Croissant et al., 2018). Two major processes which are involved in the interaction between MSNs and the membrane of RBCs are the bending of the RBC membrane to adapt to the rigid surface of MSNs and the binding of the silanol-decorated surface of MSNs with the phosphatidyl choline-containing RBC membrane. Hemolytic activity depends on several accessible surface silanol groups (Zhao et al., 2011; Yildirim et al., 2013).

3.3.1.2 Proliferation of lymphocyte population

Decreasing levels of mitotic indices and inhibited progression of cells from the G1 to the S phase of the cell cycle are indicative of lymphocyte proliferation (Lankoff et al., 2012). Further study should target the exact molecular mechanisms of lymphocyte proliferation.

3.3.1.3 Protein corona

Proteins in media that mimic biological environments instantaneously adsorbed onto the surface of the particles and form protein corona. Protein corona has been observed in MSNs. As little time as 30 s is needed to form protein corona onto MSNs in human serum. The mostly encountered proteins in the corona are

lipoproteins, hemoglobins, and α-2-HS-glycoprotein but human serum albumin was hardly shown to be adsorbed. Soft corona and hard corona are two folds of protein adsorption. Soft corona involves loosely bound proteins that are reversibly adsorbed. Hard corona contains strongly bound proteins which are irreversibly adsorbed. Studies have shown that protein size has a crucial role in protein penetration depth inside the MSNs (Croissant et al., 2018).

3.3.2 Laboratory studies
3.3.2.1 In vivo studies

In a study, the hematotoxicity of MSNs was evaluated using uncoated MSNs, chitosan-coated MSNs, low and high molecular weight PEG-coated MSNs which were injected intravenously in mice. Acute and chronic toxicity was assessed every week for four consecutive weeks. It was found that MSNs and the chitosan-coated MSNs (C-MSNs) are similar to the control group in histological and blood chemistry in acute and chronic conditions, and no toxicity was observed after their use. However, PEG may negatively affect mice with pre-existing vascular risk. It was found that PEG coating can exacerbate pre-existing vascular conditions with 2K PEG, which causes much more toxic effects than 35K PEG. Therefore, low molecular weight PEG can increase the exacerbation of vascular injury. 2K PEG exhibits rapid clearance from the body, while 35K PEG accompany by a longer circulation time (MacCuaig et al., 2022).

According to the studies, it has been found that MSNs can be considered as a promising homeostatic agent. Male New Zealand White rabbits have been used to investigate this issue. By cutting the femoral artery and vein, uncontrolled bleeding has been created. After bleeding for 10 s, 300 mg of MSNs was applied to the injury site. After 15 s of MSNs application, the injury site has been evaluated. It was found that the use of MSNs leads to a reduction in bleeding time, blood loss, and mortality rate compared to the control group. Therefore, MSNs can effectively control lethal artery hemorrhage (Chen et al., 2016).

3.3.2.2 In vitro studies

In a study that investigated the effect of morphology and pore size of MSNs, the interaction of RBCs and serum proteins with spherical MSNs with different pore sizes (s-SPs and l-SPs) and rod-shaped (RPs-3) MSNs was evaluated. Adsorption of different proteins including human albumin, globulin, and fibrinogen on different types of MSNs was investigated. As a result, it was found that formation of absorbed human albumin and fibrinogen, while not globulin, will be affected by the pore size and morphology of the MSNs. Conformational changes in absorbed proteins can influence the saturation absorption capability. However, the properties of MSNs and proteins determine the initial uptake rate. According to the results of the hemolysis assay, it has been shown that the morphology and porosity of MSNs can affect their hemolytic activity in RBCs, which is greatly reduced by the formation of a protein crown (Ma et al., 2014).

In another study, hemolysis by nonporous and porous silica NPs was investigated. The effects of porous structure and integrity on NP-cell interaction were assessed. Ultimately, it was found that nonporous and porous silica NPs can induce membrane damage in RBCs in a concentration-dependent and size-dependent manner. MSNs have induced less hemolysis compared to their nonporous

counterparts of similar size, which is probably the result of fewer silanol groups present on the cell-contactable surface in MSNs. In MSNs, pore stability can be considered as an important factor in determining hemolytic activity (Lin and Haynes, 2010).

MSNs can be considered as homeostatic agents. MSNs with larger pore size and higher specific surface area can probably exhibit better hemostatic efficacy. However, the presence of high concentrations of polar silanol groups and negative charges on MSN surfaces can also be beneficial for blood coagulation since they can be effective in activating factor XII and other coagulation proteins (Hata et al., 2014; Yoshida et al., 2015). Particle morphology, sizes, surface potential, and specific surface area can be mentioned among the factors that can be effective in the coagulating response of MSNs (Ostomel et al., 2006; Tenzer et al., 2011; Du et al., 2013; Kushida et al., 2014; Yoshida et al., 2015). In a study to determine the effect of pore size and particle size of MSNs on coagulation ability, clotting blood tests, blood coagulation factor XII adsorption, prothrombin time (PT), activated partial thromboplastin time (aPTT) and thromboelastograph were analyzed. The results of the clotting blood tests test indicated that MSN pore size ranging from 5 nm to 15 nm has a great effect on the coagulation rate of rabbit plasma, and altering particle size from 60 nm to 220 nm has little effect on coagulation. Desired pore size can induce blood proteins interaction with the interior surfaces of MSN, and as a result, blood coagulation can start faster. The final result of the analysis showed that MSNs with an average pore size of about 15 nm had the best homeostatic performance (Chen et al., 2016).

In a study, the effect of MSNs morphology on RBC membrane integrity has been investigated. For this purpose, MSNs with various shapes (spherical and rod-shaped) and different sizes (small and large) but with similar surface and pore properties were used. It was found that all four morphologies of MSNs are hemocompatible up to the concentration of 100 μg/mL, and geometry does not have much effect on blood biocompatibility, but at higher concentrations, morphology-dependent hemolytic activity was observed. MSNs with spherical geometries, showed much lower hemolytic activity however, RBC speculation occurred significantly, which indicates damage to the plasma membrane (Joglekar et al., 2013).

The effect of geometry, pore size, and surface charge of MSNs on cellular toxicity and hemolytic activity has been considered. In this study, Nonporous Stöber silica nanospheres, mesoporous silica nanospheres, mesoporous silica nanorods, and their cationic counterparts were assessed. It was found that cell toxicity of MSNs depends on cell type, surface charge, and pore size. The results have shown that geometry probably does not affect the level of SiO_2 association at early or extended time points. The extent of cellular interaction of the NPs was directly related to the amount of plasma membrane damage. It was also found that hemolytic activity was dependent on geometry, porosity, and surface charge (Yu et al., 2011).

Another study investigated the interactions of a series of MSNs [with different functional groups (polar, neutral, ionic, and hydrophobic)] with blood components. Hemolytic activity, thrombogenicity, and absorption of blood proteins on surfaces of MSNs were examined. The results of the hemolysis assay indicated that surface functionalization can decrease or avoid the hemolytic activity of naked MSNs. In order to investigate thrombogenicity, PT

and aPTT were evaluated and it was determined that the used MSNs could not show significant thrombogenic activity. Non-specific protein adsorption on MSN surfaces has also been investigated using gamma globulins and human albumin. Results indicated that surface functionalization via different ionic groups can profoundly decrease protein adsorption (Yildirim et al., 2013).

Protein corona is an emerging concept that is related to the manifestation of energetically driven protein-NP interactions and can be pretty effective in evaluating the toxicity of nanomaterials. In a study, the effect of protein formation during hemolysis induced by spherical MSNs with exposed silanol groups was investigated. Finally, it was found that human blood proteins including human plasma, albumin, hemoglobin, and RBC lysate can suppress the hemolytic effects caused by MSNs in a dose-dependent manner. In general, this study has indicated that hematotoxicity, and bioreactivity of MSNs is highly associated with protein corona formation (Martinez et al., 2015).

3.3.3 Proposed solutions to reduce MSNs blood toxicity

It is essential to minimize the cytotoxic effects of MSNs to develop drug delivery. The surface chemistry of MSNs is a predominant factor that determines the interaction of MSNs with blood cells. Hemocompatibility of MSNs can be improved by bilayer coating of MSNs which mimics bilayer composition in the outer membrane of RBCs. The majority of the outer membrane of RBC is constituted by choline lipids. The negatively-charged MSNs and the choline-based lipids interactions may cause hemolysis. It seems that lipid bilayer-coated MSNs can interface with RBC without damaging the cells (Yildirim et al., 2013; Roggers et al., 2014). An MSN which is treated with organosilane monomers prevents hemolytic activity. MSNs with aminopropyl and methyl phosphonate propyl functional groups reduce protein adsorption on their surfaces. Additionally, higher concentrations of MSNs may cause morphology-dependent hemolytic activity. Spherical geometry has better hemocompatibility than tubular morphology (Joglekar et al., 2013). However, since the interaction between biological systems and MSNs is much more complicated, thus clinical studies need to be carried out in order to provide a more vivid interaction mechanism (Yildirim et al., 2013).

The potential effects of the route of administration, particle size, and dose on the hematotoxicity of MSNs are presented in Table 3.

4 Discussion

4.1 Physicochemical factors influencing MSNs toxicity

4.1.1 MSN surface functionalization and related toxicities

MSN functionalization using PEG grafting showed lower liver, spleen, and lung uptakes in the MSN nanoparticles with the same particle sizes (Kolimi et al., 2023). In this regard, surface functionalization profoundly affects the bio-distribution of the nanoparticles and the fate of the MSN-based delivery systems. Surface functionalization also affects drug loading capacity and release kinetics (Wang et al., 2022). According to the published studies surface functionalization by N-isopropylacrylamide-co-

TABLE 3 The effect of route of administration, particle size, and dose on the hematotoxicity of MSNs.

Nanoparticles	Type of study	Rout of administration	Particle size	Dose	Exposure time	Result	Ref.
MSNs	Animal study (CD-1 female mice)	Intravenous tail injection	-MSN: 25.8 nm	10^{10} particles in 100 μL	-acute:24 h		MacCuaig et al. (2022)
			-Chitosan-MSN: 31.8 nm		- chronic: 1 injection per week for 4 weeks	-Chitosan-coated MSNs accompanied minimal toxicity.	
			-2KPEG-MSN: 29.7 nm			-PEG-coated MSNs exacerbate the pre-existing vascular conditions	
			−35KPEG-MSN: 30.1 nm				
MSNs	In vitro (Human blood samples)		- s-SPs: 67 ± 3 nm	600 μL of 0.83 mg/mL MSNs	5, 10, 20, 40, and 80 min	-The formation of absorbed human albumin and fibrinogen affected by the porosity and morphology of the MSNs	Ma et al. (2014)
			- l-SPs: 68 ± 4 nm			-The size, porosity, and morphology of MSNs could affect hemolytic activity	
			-RPs-3: (107 ± 8) × (343 ± 16)				
MSNs	In vitro (Human blood samples)		25, 42, 93, 155, and 225 nm	at a range of concentrations from 3.125 to 1600 μg/mL	3 h	-Reduced hemolytic activity of MSNs in comparison to nonporous counterparts.	Lin and Haynes (2010)
MSNs	In vitro (New Zealand rabbits blood samples)		60, 100, 150, 220 nm	Different concentration in different tests	Different exposures time in different tests	-Use of MSNs led to a reduction in bleeding time, blood loss and mortality rate.	Chen et al. (2016)
						-MSNs can effectively control lethal artery hemorrhage.	
MSNs	Animal study (Male New Zealand White rabbits)	applied over the location of injury (femoral artery and vein)	60 nm	300 mg	15 s	-Decrease bleeding time	Chen et al. (2016)
						-Decrease blood loss	
						-Decrease mortality rate	
MSNs	In vitro (Human blood samples)		- LS: 459 nm	20, 50, 100, 250 and 500 μg/mL	2 h	-Hemocompatibility is shape- and concentration-dependent	Joglekar et al. (2013)
			- SS: 275 nm				
			-LT:164,930 nm				
			-ST:142, 396 nm				
MSNs	In vitro (A549 cells or RAW 264.7 macrophages)		Have diameter of 120 nm with an aspect ratio of 2, 4 and 8 (width by length 80 × 200 nm, 150 × 600 nm and 130 × 1000 nm, respectively)	Different concentration in different tests	Different exposures time in different tests	-Cell-type-, surface charge- and pore size-dependent cellular toxicity.	Yu et al. (2011)
						-The level of cellular association of the nanoparticles has been directly related to the amount of plasma membrane damage.	
						-Hemolytic activity was shape-dependent	

TABLE 3 (*Continued*) The effect of route of administration, particle size, and dose on the hematotoxicity of MSNs.

Nanoparticles	Type of study	Rout of administration	Particle size	Dose	Exposure time	Result	Ref.
MSNs	*In vitro* (Human blood samples)		Different types of MSNs in the range of 62 to 83 nm	Different concentration in different tests	Different exposures time in different tests	-MSN surface functionalization reduced hemolytic activity -MSNs showed no significant thrombogenic activity. -MSN surface functionalization with ionic groups can affect protein adsorption	Yildirim et al. (2013)
MSNs	*In vitro* (Human blood samples)		The size is different based on the duration of intubation.	5.0, 25, 50, 125, 250, 375, and 500 µg/mL	3, 15, 45, and 60 min	-Human blood proteins and RBC lysate can reduce hemolytic activity.	Martinez et al. (2015)

methacrylic acid resulted in longer systemic circulation with lower cardiac and renal accumulation that would be accompanied by lower cardiac and renal toxicity and in this regard not only longer systemic circulation would be expectable but also lower toxicities in some vital organs would be possible (Zhang et al., 2012; Fu et al., 2013). Probably surface functionalization affects particle opsonization and that in turn will influence the fate of the nanoparticles in the systemic circulation. Surface functionalization by amine, phosphate, or carboxylic acid groups not only affects the loading capacity and loading efficacy but also influences the absorption rates and bioavailability of active pharmaceuticals (Shen et al., 2011; Shah and Rajput, 2019). Positively charged MSN nanoparticles showed higher internalization rates (Gao et al., 2019).

4.1.2 MSN particle size and related toxicities

An increase in MSN particle size resulted in limited systemic availability due to a higher tendency to accumulate within the spleen and liver (He et al., 2011). Also, skin permeation of the MSN NPs would be size-dependent (Huang et al., 2011). Smaller particles with a size range of about 42 nm showed considerable skin permeation than the larger sizes of about 75 nm. Also, particles specific surface area provides more opportunity for higher drug loading and then could enhance the dissolution rates of the poorly soluble drugs that result in higher bioavailability (Zhang et al., 2018a).

4.1.3 MSN porosity, pore size and toxicity

MSN pore size profoundly affects the release rates of the loaded drug and it seems that there is an optimum pore size for an efficient release rate that would be customized based on the specific delivery system characteristics (Chung et al., 2007; Peng et al., 2022). Based on the published reports larger pore size accompanied by higher loading capacity (Garbuzenko et al., 2014; Peng et al., 2022).

4.1.4 MSN particles shape, morphology and toxicity

MSN with different morphology showed a different rates of absorption from the GI tract and also biodegradation rates of MSN nanoparticles were not only affected by surface functionalization but also influenced by particle morphology (Rancan et al., 2012; Gao et al., 2019). Bio-distribution of the MSN nanoparticles would be affected by the morphology of the particles. In this regard, targeting of a specific tissue or organ would be tuned by adjusting the particle size and shape (Mellaerts et al., 2007).
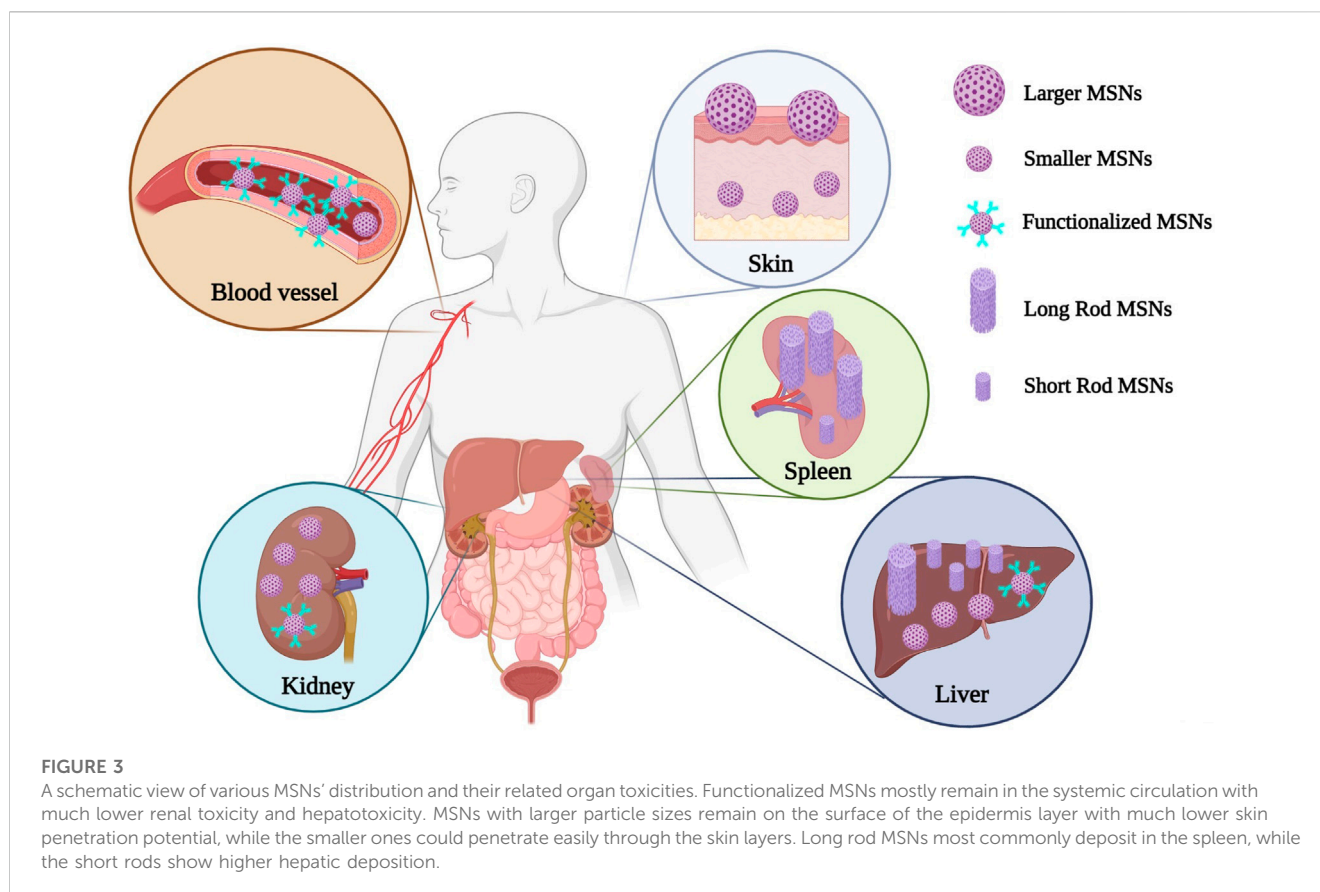
4.1.5 MSNs characteristics, toxicity and biocompatibility

Compared to nonporous silica nanoparticles, MSNs have well-defined structures, having high specific surface area, and large pore size, which have created their special capabilities (Jafari et al., 2019). MSNs are generally considered biocompatible while they may have minimal non-specific adverse effects. Various factors such as shape, size, surface modification, *etc.*, may affect the biocompatibility of MSNs. Therefore, any alteration in any of these factors may affect the toxicity caused by MSNs (Jafari et al., 2019; Niculescu, 2020). Herein, we discuss the possible modifications which can reduce MSNs associated toxicities.

4.1.6 Surface modifications of MSNs and toxicity

Since the MSNs are used to deliver encapsulated cargo to a target organ in the body, a stimuli-responsive gatekeeper would be used to induce MSNs specificity. The gatekeeper can provide stimuli responsivity for cargo release and can also circumvent toxicity. The gatekeepers on the surface of the MSNs can give them the ability of site-specific delivery, while non-coated MSNs can lead to pro-inflammatory and toxic responses, especially through the accumulation in the kidney and liver (Marzaioli et al., 2014; Mahmoud et al., 2019a). Therefore, adding gatekeeper molecules to the surface of MSNs provides specificity for drug delivery and also reduces toxicity concerns with loaded drug (Frickenstein et al., 2021).

The biocompatibility of MSNs is influenced by the silanol groups on their outer layer, which can negatively interact with biological molecules and destroy their structure. Therefore, it is important to pay attention to surface functionalization to increase biocompatibility (SlowingWu et al., 2009; Niculescu, 2020). Functional group modification is a known method to modify MSN cellular interactions. For example, amine functional groups can be substituted instead of the silanol groups to achieve the net

FIGURE 3
A schematic view of various MSNs' distribution and their related organ toxicities. Functionalized MSNs mostly remain in the systemic circulation with much lower renal toxicity and hepatotoxicity. MSNs with larger particle sizes remain on the surface of the epidermis layer with much lower skin penetration potential, while the smaller ones could penetrate easily through the skin layers. Long rod MSNs most commonly deposit in the spleen, while the short rods show higher hepatic deposition.

positive surface charge (Shi et al., 2019b). It has been found that MSNs with carboxyl or amine groups can result in less immune cells cytotoxicity than unmodified MSNs (Nabeshi et al., 2011). MSNs possessing amine and phosphate groups on their surface can exhibit mitigated pro-inflammatory responses that can be induced by naked MSNs or even PEG-conjugated MSNs (Marzaioli et al., 2014). Aminopropyl- and vinyl-modified MSNs have shown less cytotoxic effect than unmodified MSNs related to protecting blood lymphocytes from damage (Lankoff et al., 2012). It has also been found that MSNs grafted with phosphonate groups, despite having a negative charge, have been able to improve drug delivery to tumor cells, while showing limited undesirable cytotoxicity or opsonization (Yildirim et al., 2013; Bouchoucha et al., 2016).

4.1.7 Surface charge of MSNs and toxicity

The surface charge of MSNs is considered as one of the parameters that can influence their biological impacts. In general, it has been shown that the ROS-induced toxicity in positively charged (cationic) MSNs is higher than in negatively charged (anionic) and neutral MSNs (Tarn et al., 2013). It is expected that amine-modified MSNs, which have cationic surface charges, are more toxic than unmodified particles (Yu et al., 2011; Hosseinpour et al., 2020). MSNs with cationic charges may produce remarkable immune reactions and toxicity but they are desiring for trans-vascular transport in tumors. Usually, negative zeta potential may involve in serum opsonization (Niculescu, 2020).

An important point to consider is that the methods chosen for the synthesis of MSNs can influence their surface charge since based on the methods used siloxanes, silanols, or their derivatives can be put on the surface of MSNs. For example, amorphous SNPs synthesized using the wet chemistry technique are less likely to exert toxic effects on cells because they are rich on silanol groups (Sulpizi et al., 2012; Hosseinpour et al., 2020).

4.1.8 Shape, size, and density of MSNs and toxicity

It has also been found that the shape of MSNs can affect their toxicity by influencing intracellular levels of ROS (Hosseinpour et al., 2020). The shape of MSNs can also affect biocompatibility, bio-distribution, and clearance. Instantly, short-rod MSNs are mainly distributed in the liver, while long-rod MSNs are accumulated in the spleen and show a reduced elimination rate (Huang et al., 2011). A study has shown that as the aspect ratio increases, *in vivo* biodegradation, systematic absorption, and elimination will decrease. Moreover, MSNs trigger shape-dependent renal damage during the period of urinary excretion (Li et al., 2015b).

There are two opinions about the influence of the size of MSNs on biocompatibility. One opinion considers particle size as one of the most important properties and the other one has the opposite view that believes that particle size does not have any significant effect. Therefore, no precise conclusion can be reached at this point. A study has shown that MSNs of all different sizes mostly distribute in the liver and spleen, and minimally in the lung, kidney and heart. As particle size increases from 80–120–200 nm, liver, and spleen

distribution increases. The particles with an average size of 360 nm have shown different degrees of distribution in the spleen. The smaller-size NPs have longer blood-circulation lifetimes and increased particle size remarkably increases urine excretion (Tang et al., 2012). A schematic view of various MSNs' distribution and their related organ toxicities is depicted in Figure 3.

Compared to nonporous silica nanoparticles, MSNs exhibit fewer hemolytic effects, which is the result of the lower density of silanol groups decorated on the surface of MSNs (Jafari et al., 2019).

5 Conclusion

MSNs have been considered as promising drug delivery systems due to their unique characteristics including biocompatibility, high drug loading capacity, controlled drug release, and longer blood circulation time. Various physicochemical characteristics of MSNs can influence their pharmacokinetic and toxicokinetic properties which govern the disposition of MSNs in the body. In conclusion, although MSNs have been considered as relatively safe nanocarriers for drug delivery purposes, however, different levels of toxicities in main organs including the liver, kidney, and hematopoietic system may occur depending on the MSNs' size, morphology, surface functionalization, zeta potential, and routes of administration. The extent of the adverse reactions and their severity would be different based on the aforementioned MSNs characteristics and in this regard, in each case separate pharmacokinetic and toxicity studies are required to elucidate pharmacokinetic parameters and possible toxicity levels to fulfill safe administration requirements of this delivery system. A probable limitation of this review study might be that we mainly focused on MSNs utilized in the field of nanotechnology for drug delivery purposes, however, other applications of MSNs have not been discussed in detail.

6 Future perspectives

Although numerous articles have been published regarding various applications of MSNs especially for targeted delivery purposes in nano- and bio-medical fields, however, to the best of our knowledge, there is no comprehensive review on the effect of various physicochemical properties of MSNs including particle size, particle shape, specific surface area, particle charge, pore sizes, and surface functionalization on pharmacokinetic aspects and also potential toxicities of MSNs through different routes of administration. Therefore, precise consideration of the effect of each of these physicochemical parameters on pharmacokinetic and toxicokinetic aspects of MSNs would be essential for all researchers in the field of chemistry, nanotechnology,

nanomedicine, biomedicine, drug delivery, and toxicology who are working on MSNs synthesis, preparation, optimization, characterization, and also animal or clinical assessments. In addition, further assessment of the pharmacokinetic and toxicokinetic profiles of MSNs with unique properties and various surface modifications would be crucial in order to obtain an optimum clinical response and avoid unwanted adverse reactions. On the other hand, due to the mutual effects of these parameters, considering design of experiment (DOE) would be more helpful to assess the simultaneous effects of all these parameters in one study.

Data availability statement

The original contributions presented in the study are included in the article/Supplementary Material, further inquiries can be directed to the corresponding author.

Author contributions

UN contributed to Methodology; Data curation and Writing–original draft. NF contributed to Conceptualization; Methodology; Data curation; Writing–original draft and Writing–review and editing. GG contributed to Data curation and Writing–original draft. BH contributed to Data curation and Writing–original draft. PG contributed to Data curation; Writing–original draft and Writing–review and editing. SM-S contributed to Conceptualization; Methodology; Project administration, Supervision; Data curation; Writing–original draft and Writing–review and editing. All authors contributed to the article and approved the submitted version.

Conflict of interest

Publisher's note

References

Alhaithloul, H. A., Alotaibi, M. F., Bin-Jumah, M., Elgebaly, H., and Mahmoud, A. M. (2019). Olea europaea leaf extract up-regulates Nrf2/ARE/HO-1 signaling and attenuates cyclophosphamide-induced oxidative stress, inflammation and apoptosis in rat kidney. *Biomed. Pharmacother.* 111, 676–685. doi:10.1016/j.biopha.2018. 12.112

Baeza, A., and Vallet-Regí, M. (2020). Mesoporous silica nanoparticles as theranostic antitumoral nanomedicines. *Pharmaceutics* 12 (10), 957. doi:10.3390/pharmaceutics12100957

Barillet, S., Simon-Deckers, A., Herlin-Boime, N., Mayne-L'Hermite, M., Reynaud, C., Cassio, D., et al. (2010). Toxicological consequences of TiO2, SiC nanoparticles and

multi-walled carbon nanotubes exposure in several mammalian cell types: An *in vitro* study. *J. nanoparticle Res.* 12 (1), 61–73. doi:10.1007/s11051-009-9694-y

Basile, D. P., Anderson, M. D., and Sutton, T. A. (2012). Pathophysiology of acute kidney injury. *Compr. Physiol.* 2 (2), 1303–1353. doi:10.1002/cphy.c110041

K. Berger and M. J. Moeller (Editors) (2014). "Mechanisms of epithelial repair and regeneration after acute kidney injury," *Seminars in nephrology* (Amsterdam, Netherlands: Elsevier).

Bouchoucha, M., Cote, M-F., C.-Gaudreault RFortin, M-A., and Kleitz, F. (2016). Size-controlled functionalized mesoporous silica nanoparticles for tunable drug release and enhanced anti-tumoral activity. *Chem. Mater.* 28 (12), 4243–4258. doi:10.1021/acs.chemmater.6b00877

Cabellos, J., Gimeno-Benito, I., Catalán, J., Lindberg, H. K., Vales, G., Fernandez-Rosas, E., et al. (2020). Short-term oral administration of non-porous and mesoporous silica did not induce local or systemic toxicity in mice. *Nanotoxicology* 14 (10), 1324–1341. doi:10.1080/17435390.2020.1818325

Cauda, V., Mühlstein, L., Onida, B., and Bein, T. (2009). Tuning drug uptake and release rates through different morphologies and pore diameters of confined mesoporous silica. *Microporous Mesoporous Mater.* 118 (1-3), 435–442. doi:10.1016/j.micromeso.2008.09.022

Chaudhary, Z., Subramaniam, S., Khan, G. M., Abeer, M. M., Qu, Z., Janjua, T., et al. (2019). Encapsulation and controlled release of resveratrol within functionalized mesoporous silica nanoparticles for prostate cancer therapy. *Front. Bioeng. Biotechnol.* 7, 225. doi:10.3389/fbioe.2019.00225

Chen, L., Deng, H., Cui, H., Fang, J., Zuo, Z., Deng, J., et al. (2018). Inflammatory responses and inflammation-associated diseases in organs. *Oncotarget* 9 (6), 7204–7218. doi:10.18632/oncotarget.23208

Chen, Q., Moghaddas, S., Hoppel, C. L., and Lesnefsky, E. J. (2008). Ischemic defects in the electron transport chain increase the production of reactive oxygen species from isolated rat heart mitochondria. *Am. J. Physiology-Cell Physiology* 294 (2), C460–C466. doi:10.1152/ajpcell.00211.2007

Chen, X., Zhouhua, W., Jie, Z., Xinlu, F., Jinqiang, L., Yuwen, Q., et al. (2015). Renal interstitial fibrosis induced by high-dose mesoporous silica nanoparticles via the NF-κB signaling pathway. *Int. J. nanomedicine* 10, 1–22. doi:10.2147/IJN.S73538

Chen, Y., Yang, W., Chang, B., Hu, H., Fang, X., and Sha, X. (2013). *In vivo* distribution and antitumor activity of doxorubicin-loaded N-isopropylacrylamide-co-methacrylic acid coated mesoporous silica nanoparticles and safety evaluation. *Eur. J. Pharm. Biopharm.* 85 (3), 406–412. doi:10.1016/j.ejpb.2013.06.015

Chen, Z., Li, F., Liu, C., Guan, J., Hu, X., Du, G., et al. (2016). Blood clot initiation by mesoporous silica nanoparticles: Dependence on pore size or particle size? *J. Mater. Chem. B* 4 (44), 7146–7154. doi:10.1039/c6tb01946c

Chen, Z., Li, X., He, H., Ren, Z., Liu, Y., Wang, J., et al. (2012). Mesoporous silica nanoparticles with manipulated microstructures for drug delivery. *Colloids Surfaces B Biointerfaces.* 95, 274–278. doi:10.1016/j.colsurfb.2012.03.012

Chou, C-C., Chen, W., Hung, Y., and Mou, C-Y. (2017). Molecular elucidation of biological response to mesoporous silica nanoparticles *in vitro* and *in vivo*. *ACS Appl. Mater. Interfaces* 9 (27), 22235–22251. doi:10.1021/acsami.7b05359

Chung, T-H., Wu, S-H., Yao, M., Lu, C-W., Lin, Y-S., Hung, Y., et al. (2007). The effect of surface charge on the uptake and biological function of mesoporous silica nanoparticles in 3T3-L1 cells and human mesenchymal stem cells. *Biomaterials* 28 (19), 2959–2966. doi:10.1016/j.biomaterials.2007.03.006

Croissant, J. G., Fatieiev, Y., Almalik, A., and Khashab, N. M. (2018). Mesoporous silica and organosilica nanoparticles: Physical chemistry, biosafety, delivery strategies, and biomedical applications. *Adv. Healthc. Mater.* 7 (4), 1700831. doi:10.1002/adhm.201700831

de la Harpe, K. M., Kondiah, P. P., Choonara, Y. E., Marimuthu, T., du Toit, L. C., and Pillay, V. (2019). The hemocompatibility of nanoparticles: A review of cell–nanoparticle interactions and hemostasis. *Cells* 8 (10), 1209. doi:10.3390/cells8101209

Dogra, P., Adolphi, N. L., Wang, Z., Lin, Y-S., Butler, K. S., Durfee, P. N., et al. (2018). Establishing the effects of mesoporous silica nanoparticle properties on *in vivo* disposition using imaging-based pharmacokinetics. *Nat. Commun.* 9 (1), 4551–4614. doi:10.1038/s41467-018-06730-z

Du, Z., Zhao, D., Jing, L., Cui, G., Jin, M., Li, Y., et al. (2013). Cardiovascular toxicity of different sizes amorphous silica nanoparticles in rats after intratracheal instillation. *Cardiovasc. Toxicol.* 13 (3), 194–207. doi:10.1007/s12012-013-9198-y

Encinas, N., Angulo, M., Astorga, C., Colilla, M., Izquierdo-Barba, I., and Vallet-Regí, M. (2019). Mixed-charge pseudo-zwitterionic mesoporous silica nanoparticles with low-fouling and reduced cell uptake properties. *Acta biomater.* 84, 317–327. doi:10.1016/j.actbio.2018.12.012

Fang, L., Zhou, H., Cheng, L., Wang, Y., Liu, F., and Wang, S. (2023). The application of mesoporous silica nanoparticles as a drug delivery vehicle in oral disease treatment. *Front. Cell. Infect. Microbiol.* 13, 1124411. doi:10.3389/fcimb.2023.1124411

Frickenstein, A. N., Hagood, J. M., Britten, C. N., Abbott, B. S., McNally, M. W., Vopat, C. A., et al. (2021). Mesoporous silica nanoparticles: Properties and strategies for enhancing clinical effect. *Pharmaceutics* 13 (4), 570. doi:10.3390/pharmaceutics13040570

Fu, C., Liu, T., Li, L., Liu, H., Chen, D., and Tang, F. (2013). The absorption, distribution, excretion and toxicity of mesoporous silica nanoparticles in mice following different exposure routes. *Biomaterials* 34 (10), 2565–2575. doi:10.1016/j.biomaterials.2012.12.043

Fubini, B., and Hubbard, A. (2003). Reactive oxygen species (ROS) and reactive nitrogen species (RNS) generation by silica in inflammation and fibrosis. *Free Radic. Biol. Med.* 34 (12), 1507–1516. doi:10.1016/s0891-5849(03)00149-7

Gao, J., Fan, K., Jin, Y., Zhao, L., Wang, Q., Tang, Y., et al. (2019). PEGylated lipid bilayer coated mesoporous silica nanoparticles co-delivery of paclitaxel and curcumin leads to increased tumor site drug accumulation and reduced tumor burden. *Eur. J. Pharm. Sci.* 140, 105070. doi:10.1016/j.ejps.2019.105070

Garbuzenko, O. B., Mainelis, G., Taratula, O., and Minko, T. (2014). Inhalation treatment of lung cancer: The influence of composition, size and shape of nanocarriers on their lung accumulation and retention. *Cancer Biol. Med.* 11 (1), 44–55. doi:10.7497/j.issn.2095-3941.2014.01.004

George, B., You, D., Joy, M. S., and Aleksunes, L. M. (2017). Xenobiotic transporters and kidney injury. *Adv. drug Deliv. Rev.* 116, 73–91. doi:10.1016/j.addr.2017.01.005

Goscianska, J., Olejnik, A., Ejsmont, A., Galarda, A., and Wuttke, S. (2021). Overcoming the paracetamol dose challenge with wrinkled mesoporous carbon spheres. *J. Colloid Interface Sci.* 586, 673–682. doi:10.1016/j.jcis.2020.10.137

Guo, Y., Gou, K., Yang, B., Wang, Y., Pu, X., Li, S., et al. (2019). Enlarged pore size chiral mesoporous silica nanoparticles loaded poorly water-soluble drug perform superior delivery effect. *Molecules* 24 (19), 3552. doi:10.3390/molecules24193552

Han, B., Pei, Z., Shi, L., Wang, Q., Li, C., Zhang, B., et al. (2020). TiO₂ nanoparticles caused DNA damage in lung and extra-pulmonary organs through ROS-activated FOXO3a signaling pathway after intratracheal administration in rats</p>. *Int. J. Nanomedicine* 15, 6279–6294. doi:10.2147/ijn.s254969

Hao, N., Li, L., Zhang, Q., Huang, X., Meng, X., Zhang, Y., et al. (2012). The shape effect of PEGylated mesoporous silica nanoparticles on cellular uptake pathway in Hela cells. *Microporous mesoporous Mater.* 162, 14–23. doi:10.1016/j.micromeso.2012.05.040

Hartono, S. B., Hadisoewignyo, L., Yang, Y., Meka, A. K., and Yu, C. (2016). Amine functionalized cubic mesoporous silica nanoparticles as an oral delivery system for curcumin bioavailability enhancement. *Nanotechnology* 27 (50), 505605. doi:10.1088/0957-4484/27/50/505605

Hata, K., Higashisaka, K., Nagano, K., Mukai, Y., Kamada, H., Tsunoda, S-i., et al. (2014). Evaluation of silica nanoparticle binding to major human blood proteins. *Nanoscale Res. Lett.* 9 (1), 668–677. doi:10.1186/1556-276x-9-668

Hayyan, M., Hashim, M. A., and AlNashef, I. M. (2016). Superoxide ion: Generation and chemical implications. *Chem. Rev.* 116 (5), 3029–3085. doi:10.1021/acs.chemrev.5b00407

He, Q., Zhang, Z., Gao, F., Li, Y., and Shi, J. (2011). *In vivo* biodistribution and urinary excretion of mesoporous silica nanoparticles: Effects of particle size and PEGylation. *small* 7 (2), 271–280. doi:10.1002/smll.201001459

Hosseinpour, S., Walsh, L. J., and Xu, C. (2020). Biomedical application of mesoporous silica nanoparticles as delivery systems: A biological safety perspective. *J. Mater. Chem. B* 8 (43), 9863–9876. doi:10.1039/d0tb01868f

Hozayen, W. G., Mahmoud, A. M., Desouky, E. M., El-Nahass, E-S., Soliman, H. A., and Farghali, A. A. (2019). Cardiac and pulmonary toxicity of mesoporous silica nanoparticles is associated with excessive ROS production and redox imbalance in Wistar rats. *Biomed. Pharmacother.* 109, 2527–2538. doi:10.1016/j.biopha.2018.11.093

Hu, X., Ding, C., Ding, X., Fan, P., Zheng, J., Xiang, H., et al. (2020). Inhibition of myeloid differentiation protein 2 attenuates renal ischemia/reperfusion-induced oxidative stress and inflammation via suppressing TLR4/TRAF6/NF-kB pathway. *Life Sci.* 256, 117864. doi:10.1016/j.lfs.2020.117864

Huang, X., Li, L., Liu, T., Hao, N., Liu, H., Chen, D., et al. (2011). The shape effect of mesoporous silica nanoparticles on biodistribution, clearance, and biocompatibility *in vivo*. *ACS Nano* 5 (7), 5390–5399. doi:10.1021/nn200365a

Hwang, J-w., Rajendrasozhan, S., Yao, H., Chung, S., Sundar, I. K., Huyck, H. L., et al. (2011). FOXO3 deficiency leads to increased susceptibility to cigarette smoke-induced inflammation, airspace enlargement, and chronic obstructive pulmonary disease. *J. Immunol.* 187 (2), 987–998. doi:10.4049/jimmunol.1001861

Itoh, K., Chiba, T., Takahashi, S., Ishii, T., Igarashi, K., Katoh, Y., et al. (1997). An Nrf2/small Maf heterodimer mediates the induction of phase II detoxifying enzyme genes through antioxidant response elements. *Biochem. biophysical Res. Commun.* 236 (2), 313–322. doi:10.1006/bbrc.1997.6943

Izquierdo-Barba, I., Sousa, E., Doadrio, J. C., Doadrio, A. L., Pariente, J. P., Martínez, A., et al. (2009). Influence of mesoporous structure type on the controlled delivery of drugs: Release of ibuprofen from MCM-48, SBA-15 and functionalized SBA-15. *J. sol-gel Sci. Technol.* 50 (3), 421–429. doi:10.1007/s10971-009-1932-3

Jafari, S., Derakhshankhah, H., Alaei, L., Fattahi, A., Varnamkhasti, B. S., and Saboury, A. A. (2019). Mesoporous silica nanoparticles for therapeutic/diagnostic applications. *Biomed. Pharmacother.* 109, 1100–1111. doi:10.1016/j.biopha.2018.10.167

Jambhrunkar, S., Qu, Z., Popat, A., Yang, J., Noonan, O., Acauan, L., et al. (2014). Effect of surface functionality of silica nanoparticles on cellular uptake and cytotoxicity. *Mol. Pharm.* 11 (10), 3642–3655. doi:10.1021/mp500385n

Joglekar, M., Roggers, R. A., Zhao, Y., and Trewyn, B. G. (2013). Interaction effects of mesoporous silica nanoparticles with different morphologies on human red blood cells. *Rsc Adv.* 3 (7), 2454–2461. doi:10.1039/c2ra22264g

Kamaly, N., He, J. C., Ausiello, D. A., and Farokhzad, O. C. (2016). Nanomedicines for renal disease: Current status and future applications. *Nat. Rev. Nephrol.* 12 (12), 738–753. doi:10.1038/nrneph.2016.156

Karaman, D. S., Desai, D., Senthilkumar, R., Johansson, E. M., Råtts, N., Odén, M., et al. (2012). Shape engineering vs organic modification of inorganic nanoparticles as a tool for enhancing cellular internalization. *Nanoscale Res. Lett.* 7 (1), 358–414. doi:10.1186/1556-276x-7-358

Karmakar, A., Zhang, Q., and Zhang, Y. (2014). Neurotoxicity of nanoscale materials. *J. Food Drug Analysis* 22 (1), 147–160. doi:10.1016/j.jfda.2014.01.012

Kolimi, P., Narala, S., Youssef, A. A. A., Nyavanandi, D., and Dudhipala, N. (2023). A systemic review on development of mesoporous nanoparticles as a vehicle for transdermal drug delivery. *Nanotheranostics* 7 (1), 70–89. doi:10.7150/ntno.77395

Krajewski, S., Prucek, R., Panacek, A., Avci-Adali, M., Nolte, A., Straub, A., et al. (2013). Hemocompatibility evaluation of different silver nanoparticle concentrations employing a modified Chandler-loop *in vitro* assay on human blood. *Acta Biomater.* 9 (7), 7460–7468. doi:10.1016/j.actbio.2013.03.016

Kushida, T., Saha, K., Subramani, C., Nandwana, V., and Rotello, V. M. (2014). Effect of nano-scale curvature on the intrinsic blood coagulation system. *Nanoscale* 6 (23), 14484–14487. doi:10.1039/c4nr04128c

L'azou, B., Jorly, J., On, D., Sellier, E., Moisan, F., Fleury-Feith, J., et al. (2008). *In vitro* effects of nanoparticles on renal cells. *Part. fibre Toxicol.* 5 (1), 22. doi:10.1186/1743-8977-5-22

Lankoff, A., Arabski, M., Wegierek-Ciuk, A., Kruszewski, M., Lisowska, H., Banasik-Nowak, A., et al. (2012). Effect of surface modification of silica nanoparticles on toxicity and cellular uptake by human peripheral blood lymphocytes *in vitro*. *Nanotoxicology* 7 (3), 235–250. doi:10.3109/17435390.2011.649796

Lee, C. H., Cheng, S. H., Huang, I. P., Souris, J. S., Yang, C. S., Mou, C. Y., et al. (2010). Intracellular pH-responsive mesoporous silica nanoparticles for the controlled release of anticancer chemotherapeutics. *Angew. Chem. Int. Ed.* 49 (44), 8214–8219. doi:10.1002/anie.201002639

Lee, J. E., Lee, N., Kim, T., Kim, J., and Hyeon, T. (2011). Multifunctional mesoporous silica nanocomposite nanoparticles for theranostic applications. *Accounts Chem. Res.* 44 (10), 893–902. doi:10.1021/ar2000259

Lee, S., Kim, M-S., Lee, D., Kwon, T. K., Khang, D., Yun, H-S., et al. (2013). The comparative immunotoxicity of mesoporous silica nanoparticles and colloidal silica nanoparticles in mice. *Int. J. nanomedicine* 8, 147–158. doi:10.2147/ijn.s39534

Levy, D. E., and Darnell, J. (2002). Stats: Transcriptional control and biological impact. *Nat. Rev. Mol. Cell Biol.* 3 (9), 651–662. doi:10.1038/nrm909

Li, J., Du, X., Zheng, N., Xu, L., Xu, J., and Li, S. (2016). Contribution of carboxyl modified chiral mesoporous silica nanoparticles in delivering doxorubicin hydrochloride *in vitro*: pH-response controlled release, enhanced drug cellular uptake and cytotoxicity. *Colloids Surfaces B Biointerfaces.* 141, 374–381. doi:10.1016/j.colsurfb.2016.02.009

Li, J., Guo, Y., Li, H., Shang, L., and Li, S. (2018). Superiority of amino-modified chiral mesoporous silica nanoparticles in delivering indometacin. *Artif. Cells, Nanomedicine, Biotechnol.* 46 (5), 1085–1094. doi:10.1080/21691401.2017.1360326

Li, J., Sun, R., Xu, H., and Wang, G. (2022). Integrative metabolomics, proteomics and transcriptomics analysis reveals liver toxicity of mesoporous silica nanoparticles. *Front. Pharmacol.* 13, 835359. doi:10.3389/fphar.2022.835359

Li, J., Xu, L., Wang, H., Yang, B., Liu, H., Pan, W., et al. (2016). Comparison of bare and amino modified mesoporous silica@ poly (ethyleneimine) s xerogel as indomethacin carrier: Superiority of amino modification. *Mater. Sci. Eng. C* 59, 710–716. doi:10.1016/j.msec.2015.10.072

Li, L., Liu, T., Fu, C., Tan, L., Meng, X., and Liu, H. (2015). Biodistribution, excretion, and toxicity of mesoporous silica nanoparticles after oral administration depend on their shape. *Nanomedicine Nanotechnol. Biol. Med.* 11 (8), 1915–1924. doi:10.1016/j.nano.2015.07.004

Li, L., Liu, T., Fu, C., Tan, L., Meng, X., Liu, H. J. N. N., et al. (2015). Biodistribution, excretion, and toxicity of mesoporous silica nanoparticles after oral administration depend on their shape. *Nanomedicine* 11(8), 1915–1924. doi:10.1016/j.nano.2015.07.004

Li, Y., and Ju, D. (2018). The role of autophagy in nanoparticles-induced toxicity and its related cellular and molecular mechanisms. *Cell. Mol. Toxicol. Nanoparticles* 1048, 71–84. doi:10.1007/978-3-319-72041-8_5

Li, Z., Barnes, J. C., Bosoy, A., Stoddart, J. F., and Zink, J. I. (2012). Mesoporous silica nanoparticles in biomedical applications. *Chem. Soc. Rev.* 41 (7), 2590–2605. doi:10.1039/c1cs15246g

Lin, Y-S., and Haynes, C. L. (2010). Impacts of mesoporous silica nanoparticle size, pore ordering, and pore integrity on hemolytic activity. *J. Am. Chem. Soc.* 132 (13), 4834–4842. doi:10.1021/ja910846q

Lindén, M. (2018). Biodistribution and excretion of intravenously injected mesoporous silica nanoparticles: Implications for drug delivery efficiency and safety. *Enzym.* 43, 155–180. doi:10.1016/bs.enz.2018.07.007

Liu, T., Li, L., Fu, C., Liu, H., Chen, D., and Tang, F. (2012). Pathological mechanisms of liver injury caused by continuous intraperitoneal injection of silica nanoparticles. *Biomaterials* 33 (7), 2399–2407. doi:10.1016/j.biomaterials.2011.12.008

Lundvig, D. M., Immenschuh, S., and Wagener, F. A. (2012). Heme oxygenase, inflammation, and fibrosis: The good, the bad, and the ugly? *Front. Pharmacol.* 3, 81. doi:10.3389/fphar.2012.00081

Ma, Z., Bai, J., Wang, Y., and Jiang, X. (2014). Impact of shape and pore size of mesoporous silica nanoparticles on serum protein adsorption and RBCs hemolysis. *ACS Appl. Mater. interfaces* 6 (4), 2431–2438. doi:10.1021/am404860q

MacCuaig, W. M., Samykutty, A., Foote, J., Luo, W., Filatenkov, A., Li, M., et al. (2022). Toxicity assessment of mesoporous silica nanoparticles upon intravenous injection in mice: Implications for drug delivery. *Pharmaceutics* 14 (5), 969. doi:10.3390/pharmaceutics14050969

Mahmoud, A. M., Desouky, E. M., Hozayen, W. G., Bin-Jumah, M., El-Nahass, E-S., Soliman, H. A., et al. (2019). Mesoporous silica nanoparticles trigger liver and kidney injury and fibrosis via altering TLR4/NF-κB, JAK2/STAT3 and Nrf2/HO-1 signaling in rats. *Biomolecules* 9 (10), 528. doi:10.3390/biom9100528

Mahmoud, A. M., Germoush, M. O., Al-Anazi, K. M., Mahmoud, A. H., Farah, M. A., and Allam, A. A. (2018). Commiphora molmol protects against methotrexate-induced nephrotoxicity by up-regulating Nrf2/ARE/HO-1 signaling. *Biomed. Pharmacother.* 106, 499–509. doi:10.1016/j.biopha.2018.06.171

Mahmoud, A. M., Hussein, O. E., Abd El-Twab, S. M., and Hozayen, W. G. (2019). Ferulic acid protects against methotrexate nephrotoxicity via activation of Nrf2/ARE/HO-1 signaling and PPARγ, and suppression of NF-κB/NLRP3 inflammasome axis. *Food & Funct.* 10 (8), 4593–4607. doi:10.1039/c9fo00114j

Manzano, M., and Vallet-Regí, M. (2018). Mesoporous silica nanoparticles in nanomedicine applications. *J. Mater. Sci. Mater. Med.* 29 (5), 65–14. doi:10.1007/s10856-018-6069-x

Martinez, D. S. T., Paula, A. J., Fonseca, L. C., Luna, L. A. V., Silveira, C. P., Durán, N., et al. (2015). Monitoring the hemolytic effect of mesoporous silica nanoparticles after human blood protein corona formation. *Eur. J. Inorg. Chem.* 2015 (27), 4595–4602. doi:10.1002/ejic.201500573

Marzaioli, V., Aguilar-Pimentel, J. A., Weichenmeier, I., Luxenhofer, G., Wiemann, M., Landsiedel, R., et al. (2014). Surface modifications of silica nanoparticles are crucial for their inert versus proinflammatory and immunomodulatory properties. *Int. J. nanomedicine* 9, 2815–2832. doi:10.2147/IJN.S57396

Matus, M. F., Vilos, C., Cisterna, B. A., Fuentes, E., and Palomo, I. (2018). Nanotechnology and primary hemostasis: Differential effects of nanoparticles on platelet responses. *Vasc. Pharmacol.* 101, 1–8. doi:10.1016/j.vph.2017.11.004

Mehmood, Y., Khan, I. U., Shahzad, Y., Khan, R. U., Iqbal, M. S., Khan, H. A., et al. (2020). *In-vitro* and *in-vivo* evaluation of velpatasvir-loaded mesoporous silica scaffolds. A prospective carrier for drug bioavailability enhancement. *Pharmaceutics* 12 (4), 307. doi:10.3390/pharmaceutics12040307

Mellaerts, R., Aerts, C. A., Van Humbeeck, J., Augustijns, P., Van den Mooter, G., and Martens, J. A. (2007). Enhanced release of itraconazole from ordered mesoporous SBA-15 silica materials. *Chem. Commun.* 13, 1375–1377. doi:10.1039/b616746b

Meng, H., Xue, M., Xia, T., Ji, Z., Tarn, D. Y., Zink, J. I., et al. (2011). Use of size and a copolymer design feature to improve the biodistribution and the enhanced permeability and retention effect of doxorubicin-loaded mesoporous silica nanoparticles in a murine xenograft tumor model. *ACS Nano* 5 (5), 4131–4144. doi:10.1021/nn200809t

Milić, M., Leitinger, G., Pavičić, I., Zebić Avdičević, M., Dobrović, S., Goessler, W., et al. (2015). Cellular uptake and toxicity effects of silver nanoparticles in mammalian kidney cells. *J. Appl. Toxicol.* 35 (6), 581–592. doi:10.1002/jat.3081

Mirshafiee, V., Jiang, W., Sun, B., Wang, X., and Xia, T. (2017). Facilitating translational nanomedicine via predictive safety assessment. *Mol. Ther.* 25 (7), 1522–1530. doi:10.1016/j.ymthe.2017.03.011

Mohammadinejad, R., Moosavi, M. A., Tavakol, S., Vardar, D. Ö., Hosseini, A., Rahmati, M., et al. (2019). Necrotic, apoptotic and autophagic cell fates triggered by nanoparticles. *Autophagy* 15 (1), 4–33. doi:10.1080/15548627.2018.1509171

Mohammadpour, R., Cheney, D. L., Grunberger, J. W., Yazdimamaghani, M., Jedrzkiewicz, J., Isaacson, K. J., et al. (2020). One-year chronic toxicity evaluation of single dose intravenously administered silica nanoparticles in mice and their *ex vivo* human hemocompatibility. *J. Control. Release* 324, 471–481. doi:10.1016/j.jconrel.2020.05.027

Mohammadpour, R., Yazdimamaghani, M., Cheney, D. L., Jedrzkiewicz, J., and Ghandehari, H. (2019). Subchronic toxicity of silica nanoparticles as a function of size and porosity. *J. Control. Release* 304, 216–232. doi:10.1016/j.jconrel.2019.04.041

Møller, P., Jacobsen, N. R., Folkmann, J. K., Danielsen, P. H., Mikkelsen, L., Hemmingsen, J. G., et al. (2010). Role of oxidative damage in toxicity of particulates. *Free Radic. Res.* 44 (1), 1–46. doi:10.3109/10715760903300691

Morrow, B., and McFarlan, A. (1992). Surface vibrational modes of silanol groups on silica. *J. Phys. Chem.* 96 (3), 1395–1400. doi:10.1021/j100182a068

Murugadoss, S., Lison, D., Godderis, L., Van Den Brule, S., Mast, J., Brassinne, F., et al. (2017). Toxicology of silica nanoparticles: An update. *Archives Toxicol.* 91 (9), 2967–3010. doi:10.1007/s00204-017-1993-y

Nabeshi, H., Yoshikawa, T., Arimori, A., Yoshida, T., Tochigi, S., Hirai, T., et al. (2011). Effect of surface properties of silica nanoparticles on their cytotoxicity and cellular distribution in murine macrophages. *Nanoscale Res. Lett.* 6 (1), 93–96. doi:10.1186/1556-276x-6-93

Nemmar, A., Yuvaraju, P., Beegam, S., Yasin, J., Kazzam, E. E., and Ali, B. H. (2016). Oxidative stress, inflammation, and DNA damage in multiple organs of mice acutely exposed to amorphous silica nanoparticles. *Int. J. nanomedicine* 11, 919–928. doi:10.2147/ijn.s92278

Nho, R. S., and Hergert, P. (2014). FoxO3a and disease progression. *World J. Biol. Chem.* 5 (3), 346. doi:10.4331/wjbc.v5.i3.346

Niculescu, V-C. (2020). Mesoporous silica nanoparticles for bio-applications. *Front. Mater.* 7, 36. doi:10.3389/fmats.2020.00036

Ogata, H., Chinen, T., Yoshida, T., Kinjyo, I., Takaesu, G., Shiraishi, H., et al. (2006). Loss of SOCS3 in the liver promotes fibrosis by enhancing STAT3-mediated TGF-β1 production. *Oncogene* 25 (17), 2520–2530. doi:10.1038/sj.onc.1209281

Ostomel, T. A., Shi, Q., and Stucky, G. D. (2006). Oxide hemostatic activity. *J. Am. Chem. Soc.* 128 (26), 8384–8385. doi:10.1021/ja061717a

Pandita, D., Munjal, A., Poonia, N., Awasthi, R., Kalonia, H., and Lather, V. (2021). Albumin-coated mesoporous silica nanoparticles of docetaxel: Preparation, characterization, and pharmacokinetic evaluation. *ASSAY Drug Dev. Technol.* 19 (4), 226–236. doi:10.1089/adt.2020.1039

Passagne, I., Morille, M., Rousset, M., Pujalté, I., and L'azou, B. (2012). Implication of oxidative stress in size-dependent toxicity of silica nanoparticles in kidney cells. *Toxicology* 299 (2-3), 112–124. doi:10.1016/j.tox.2012.05.010

Peng, H., Xu, Z., Wang, Y., Feng, N., Yang, W., and Tang, J. (2020). Biomimetic mesoporous silica nanoparticles for enhanced blood circulation and cancer therapy. *ACS Appl. Bio Mater.* 3 (11), 7849–7857. doi:10.1021/acsabm.0c01014

Peng, S., Huang, B., Lin, Y., Pei, G., and Zhang, L. (2022). Effect of surface functionalization and pore structure type on the release performance of mesoporous silica nanoparticles. *Microporous Mesoporous Mater.* 336, 111862. doi:10.1016/j.micromeso.2022.111862

Peretti, E., Miletto, I., Stella, B., Rocco, F., Berlier, G., and Arpicco, S. (2018). Strategies to obtain encapsulation and controlled release of pentamidine in mesoporous silica nanoparticles. *Pharmaceutics* 10 (4), 195. doi:10.3390/pharmaceutics10040195

Qian, Q. (2017). Inflammation: A key contributor to the Genesis and progression of chronic kidney disease. *Expand. Hemodial.* 191, 72–83. doi:10.1159/000479257

Qu, F., Zhu, G., Huang, S., Li, S., Sun, J., Zhang, D., et al. (2006). Controlled release of Captopril by regulating the pore size and morphology of ordered mesoporous silica. *Microporous Mesoporous Mater.* 92 (1-3), 1–9. doi:10.1016/j.micromeso.2005.12.004

Racanelli, V., and Rehermann, B. (2006). The liver as an immunological organ. *Hepatology* 43 (S1), S54–S62. doi:10.1002/hep.21060

Rancan, F., Gao, Q., Graf, C., Troppens, S., Hadam, S., Hackbarth, S., et al. (2012). Skin penetration and cellular uptake of amorphous silica nanoparticles with variable size, surface functionalization, and colloidal stability. *ACS Nano* 6 (8), 6829–6842. doi:10.1021/nn301622h

Ranucci, M., Ballotta, A., Di Dedda, U., Bayshnikova, E., Dei Poli, M., Resta, M., et al. (2020). The procoagulant pattern of patients with COVID-19 acute respiratory distress syndrome. *J. Thrombosis Haemostasis* 18, 1747–1751. doi:10.1111/jth.14854

Rascol, E., Pisani, C., Dorandeu, C., Nyalosaso, J. L., Charnay, C., Daurat, M., et al. (2018). Biosafety of mesoporous silica nanoparticles. *Biomimetics* 3 (3), 22. doi:10.3390/biomimetics3030022

Reddy, U. A., Prabhakar, P., and Mahboob, M. (2017). Biomarkers of oxidative stress for *in vivo* assessment of toxicological effects of iron oxide nanoparticles. *Saudi J. Biol. Sci.* 24 (6), 1172–1180. doi:10.1016/j.sjbs.2015.09.029

Ren, Q., Guo, F., Tao, S., Huang, R., Ma, L., and Fu, P. (2020). Flavonoid fisetin alleviates kidney inflammation and apoptosis via inhibiting Src-mediated NF-κB p65 and MAPK signaling pathways in septic AKI mice. *Biomed. Pharmacother.* 122, 109772. doi:10.1016/j.biopha.2019.109772

Reshma, V., and Mohanan, P. (2017). Cellular interactions of zinc oxide nanoparticles with human embryonic kidney (HEK 293) cells. *Colloids Surfaces B Biointerfaces.* 157, 182–190. doi:10.1016/j.colsurfb.2017.05.069

Ritz, S., Schöttler, S., Kotman, N., Baier, G., Musyanovych, A., Kuharev, Jr, et al. (2015). Protein corona of nanoparticles: Distinct proteins regulate the cellular uptake. *Biomacromolecules* 16 (4), 1311–1321. doi:10.1021/acs.biomac.5b00108

Roggers, R. A., Joglekar, M., Valenstein, J. S., and Trewyn, B. G. (2014). Mimicking red blood cell lipid membrane to enhance the hemocompatibility of large-pore mesoporous silica. *ACS Appl. Mater. interfaces* 6 (3), 1675–1681. doi:10.1021/am4045713

Sábio, R. M., Meneguin, A. B., dos Santos, A. M., Monteiro, A. S., and Chorilli, M. (2021). Exploiting mesoporous silica nanoparticles as versatile drug carriers for several routes of administration. *Microporous Mesoporous Mater.* 312, 110774. doi:10.1016/j.micromeso.2020.110774

Sapino, S., Ugazio, E., Gastaldi, L., Miletto, I., Berlier, G., Zonari, D., et al. (2015). Mesoporous silica as topical nanocarriers for quercetin: Characterization and *in vitro* studies. *Eur. J. Pharm. Biopharm.* 89, 116–125. doi:10.1016/j.ejpb.2014.11.022

Sarkar, A., Ghosh, M., and Sil, P. C. (2014). Nanotoxicity: Oxidative stress mediated toxicity of metal and metal oxide nanoparticles. *J. Nanosci. Nanotechnol.* 14 (1), 730–743. doi:10.1166/jnn.2014.8752

Saroj, S., and Rajput, S. J. (2018). Etoposide encapsulated functionalized mesoporous silica nanoparticles: Synthesis, characterization and effect of functionalization on dissolution kinetics in simulated and biorelevant media. *J. Drug Deliv. Sci. Technol.* 44, 27–40. doi:10.1016/j.jddst.2017.11.020

Satta, S., Mahmoud, A. M., Wilkinson, F. L., Yvonne Alexander, M., and White, S. J. (2017). The role of Nrf2 in cardiovascular function and disease. *Oxidative Med. Cell. Longev.* 2017. doi:10.1155/2017/9237263

Scanlon, V. C., and Sanders, T. (2018). *Essentials of anatomy and physiology.* United States: F. A. Davis.

Shadmani, N., Makvandi, P., Parsa, M., Azadi, A., Nedaei, K., Mozafari, N., et al. (2023). Enhancing methotrexate delivery in the brain by mesoporous silica nanoparticles functionalized with cell-penetrating peptide using *in vivo* and *ex vivo* monitoring. *Mol. Pharm.* 20 (3), 1531–1548. doi:10.1021/acs.molpharmaceut.2c00755

Shah, P., and Rajput, S. J. (2019). Investigation of *in vitro* permeability and *in vivo* pharmacokinetic behavior of bare and functionalized MCM-41 and MCM-48 mesoporous silica nanoparticles: A burst and controlled drug release system for raloxifene. *Drug Dev. Industrial Pharm.* 45 (4), 587–602. doi:10.1080/03639045.2019.1569028

Shen, S-C., Ng, W. K., Chia, L., Hu, J., and Tan, R. B. (2011). Physical state and dissolution of ibuprofen formulated by co-spray drying with mesoporous silica: Effect of pore and particle size. *Int. J. Pharm.* 410 (1-2), 188–195. doi:10.1016/j.ijpharm.2011.03.018

Shi, H., Liu, S., Cheng, J., Yuan, S., Yang, Y., Fang, T., et al. (2019). Charge-selective delivery of proteins using mesoporous silica nanoparticles fused with lipid bilayers. *ACS Appl. Mater. interfaces* 11 (4), 3645–3653. doi:10.1021/acsami.8b15390

Shi, W-Z., Tian, Y., and Li, J. (2019). GCN2 suppression attenuates cerebral ischemia in mice by reducing apoptosis and endoplasmic reticulum (ER) stress through the blockage of FoxO3a-regulated ROS production. *Biochem. biophysical Res. Commun.* 516 (1), 285–292. doi:10.1016/j.bbrc.2019.05.181

SlowingII, Vivero-Escoto, J. L., Trewyn, B. G., and Lin, V. S-Y. (2010). Mesoporous silica nanoparticles: Structural design and applications. *J. Mater. Chem.* 20 (37), 7924–7937. doi:10.1039/c0jm00554a

SlowingII, Wu, C. W., Vivero-Escoto, J. L., and Lin, V. S. Y. (2009). Mesoporous silica nanoparticles for reducing hemolytic activity towards mammalian red blood cells. *Small* 5 (1), 57–62. doi:10.1002/smll.200800926

Sulpizi, M., Gaigeot, M-P., and Sprik, M. (2012). The silica–water interface: How the silanols determine the surface acidity and modulate the water properties. *J. Chem. theory Comput.* 8 (3), 1037–1047. doi:10.1021/ct2007154

Sun, L., Li, Y., Liu, X., Jin, M., Zhang, L., Du, Z., et al. (2011). Cytotoxicity and mitochondrial damage caused by silica nanoparticles. *Toxicol. vitro* 25 (8), 1619–1629. doi:10.1016/j.tiv.2011.06.012

Sun, L., Sogo, Y., Wang, X., and Ito, A. (2021). Biosafety of mesoporous silica nanoparticles: A combined experimental and literature study. *J. Mater. Sci. Mater. Med.* 32 (9), 102–115. doi:10.1007/s10856-021-06582-y

Sun, Z., Yan, B., Yu, W. Y., Yao, X., Ma, X., Sheng, G., et al. (2016). Vitexin attenuates acute doxorubicin cardiotoxicity in rats via the suppression of oxidative stress, inflammation and apoptosis and the activation of FOXO3a. *Exp. Ther. Med.* 12 (3), 1879–1884. doi:10.3892/etm.2016.3518

Tang, F., Li, L., and Chen, D. J. A. (2012). Mesoporous silica nanoparticles: Synthesis, biocompatibility and drug delivery. *Adv. Mat.* 24 (12), 1504–1534. doi:10.1002/adma.201104763

Tarn, D., Ashley, C. E., Xue, M., Carnes, E. C., Zink, J. I., and Brinker, C. J. (2013). Mesoporous silica nanoparticle nanocarriers: Biofunctionality and biocompatibility. *Accounts Chem. Res.* 46 (3), 792–801. doi:10.1021/ar3000986

Tenzer, S., Docter, D., Rosfa, S., Wlodarski, A., KuharevJr, Rekik, A., et al. (2011). Nanoparticle size is a critical physicochemical determinant of the human blood plasma corona: A comprehensive quantitative proteomic analysis. *ACS Nano* 5 (9), 7155–7167. doi:10.1021/nn201950e

Thit, A., Selck, H., and Bjerregaard, H. F. (2015). Toxic mechanisms of copper oxide nanoparticles in epithelial kidney cells. *Toxicol. vitro* 29 (5), 1053–1059. doi:10.1016/j.tiv.2015.03.020

Thompson, W. L., and Takebe, T. (2021). Human liver model systems in a dish. *Dev. Growth & Differ.* 63 (1), 47–58. doi:10.1111/dgd.12708

Tsukada, S., Parsons, C. J., and Rippe, R. A. (2006). Mechanisms of liver fibrosis. *Clin. Chim. acta* 364 (1-2), 33–60. doi:10.1016/j.cca.2005.06.014

Valentini, X., Absil, L., Laurent, G., Robbe, A., Laurent, S., Muller, R., et al. (2017). Toxicity of TiO2 nanoparticles on the NRK52E renal cell line. *Mol. Cell. Toxicol.* 13 (4), 419–431. doi:10.1007/s13273-017-0046-1

Valetti, S., Thomsen, H., Wankar, J., Falkman, P., Manet, I., Feiler, A., et al. (2021). Can mesoporous nanoparticles promote bioavailability of topical pharmaceutics? *Int. J. Pharm.* 602, 120609. doi:10.1016/j.ijpharm.2021.120609

Van Speybroeck, M., Mellaerts, R., Mols, R., Do Thi, T., Martens, J. A., Van Humbeeck, J., et al. (2010). Enhanced absorption of the poorly soluble drug fenofibrate by tuning its release rate from ordered mesoporous silica. *Eur. J. Pharm. Sci.* 41 (5), 623–630. doi:10.1016/j.ejps.2010.09.002

Villeneuve, N. F., Lau, A., and Zhang, D. D. (2010). Regulation of the nrf2–keap1 antioxidant response by the ubiquitin proteasome system: An insight into cullin-ring ubiquitin ligases. *Antioxidants redox Signal.* 13 (11), 1699–1712. doi:10.1089/ars.2010.3211

Wang, F., Gao, F., Lan, M., Yuan, H., Huang, Y., and Liu, J. (2009). Oxidative stress contributes to silica nanoparticle-induced cytotoxicity in human embryonic kidney cells. *Toxicol. vitro* 23 (5), 808–815. doi:10.1016/j.tiv.2009.04.009

Wang, T., Zhang, Z., Xie, M., Li, S., Zhang, J., and Zhou, J. (2022). Apigenin attenuates mesoporous silica nanoparticles-induced nephrotoxicity by activating FOXO3a. *Biol. Trace Elem. Res.* 200 (6), 2793–2806. doi:10.1007/s12011-021-02871-3

Wang, X., Li, C., Fan, N., Li, J., He, Z., and Sun, J. (2017). Multimodal nanoporous silica nanoparticles functionalized with aminopropyl groups for improving loading and controlled release of doxorubicin hydrochloride. *Mater. Sci. Eng. C* 78, 370–375. doi:10.1016/j.msec.2017.04.060

Wang, Y., Sun, L., Jiang, T., Zhang, J., Zhang, C., Sun, C., et al. (2014). The investigation of MCM-48-type and MCM-41-type mesoporous silica as oral solid dispersion carriers for water insoluble cilostazol. *Drug Dev. industrial Pharm.* 40 (6), 819–828. doi:10.3109/03639045.2013.788013

Wang, Y., Zhao, Y., Cui, Y., Zhao, Q., Zhang, Q., Musetti, S., et al. (2018). Overcoming multiple gastrointestinal barriers by bilayer modified hollow mesoporous silica nanocarriers. *Acta Biomater.* 65, 405–416. doi:10.1016/j.actbio.2017.10.025

Wani, A., Savithra, G. H. L., Abyad, A., Kanvinde, S., Li, J., Brock, S., et al. (2017). Surface PEGylation of Mesoporous Silica Nanorods (MSNR): Effect on loading, release, and delivery of mitoxantrone in hypoxic cancer cells. *Sci. Rep.* 7 (1), 2274–2311. doi:10.1038/s41598-017-02531-4

Waters, K. M., Masiello, L. M., Zangar, R. C., Tarasevich, B. J., Karin, N. J., Quesenberry, R. D., et al. (2009). Macrophage responses to silica nanoparticles are highly conserved across particle sizes. *Toxicol. Sci.* 107 (2), 553–569. doi:10.1093/toxsci/kfn250

Winkler, H. C., Kornprobst, J., Wick, P., von Moos, L. M., Trantakis, I., Schraner, E. M., et al. (2017). MyD88-dependent pro-interleukin-1β induction in dendritic cells exposed to food-grade synthetic amorphous silica. *Part. fibre Toxicol.* 14 (1), 21–13. doi:10.1186/s12989-017-0202-8

Wolf, G., Chen, S., and Ziyadeh, F. N. (2005). From the periphery of the glomerular capillary wall toward the center of disease: Podocyte injury comes of age in diabetic nephropathy. *Diabetes* 54 (6), 1626–1634. doi:10.2337/diabetes.54.6.1626

Wu, L., Guo, C., and Wu, J. (2020). Therapeutic potential of PPARγ natural agonists in liver diseases. *J. Cell. Mol. Med.* 24 (5), 2736–2748. doi:10.1111/jcmm.15028

Xi, C., Zhou, J., Du, S., and Peng, S. (2016). Autophagy upregulation promotes macrophages to escape mesoporous silica nanoparticle (MSN)-induced NF-κB-dependent inflammation. *Inflamm. Res* 65 (4), 325–341. doi:10.1007/s00011-016-0919-0

Xiao, L., Liu, C., Chen, X., and Yang, Z. (2016). Zinc oxide nanoparticles induce renal toxicity through reactive oxygen species. *Food Chem. Toxicol.* 90, 76–83. doi:10.1016/j.fct.2016.02.002

Xu, J., Li, Z., Xu, P., Xiao, L., and Yang, Z. (2013). Nanosized copper oxide induces apoptosis through oxidative stress in podocytes. *Archives Toxicol.* 87 (6), 1067–1073. doi:10.1007/s00204-012-0925-0

Xu, P., Xu, J., Liu, S., and Yang, Z. (2012). Nano copper induced apoptosis in podocytes via increasing oxidative stress. *J. Hazard. Mater.* 241, 279–286. doi:10.1016/j.jhazmat.2012.09.041

Xue, Y., Chen, Q., Ding, T., and Sun, J. (2014). SiO- nanoparticle-induced impairment of mitochondrial energy metabolism in hepatocytes directly and through a Kupffer cell-mediated pathway *in vitro*. *Int. J. nanomedicine* 9, 2891–2903. doi:10.2147/ijn.s60661

Yamagishi, Y., Watari, A., Hayata, Y., Li, X., Kondoh, M., Yoshioka, Y., et al. (2013). Acute and chronic nephrotoxicity of platinum nanoparticles in mice. *Nanoscale Res. Lett.* 8 (1), 395–397. doi:10.1186/1556-276x-8-395

Yamamoto, Y., and Gaynor, R. B. (2001). Role of the NF-kB pathway in the pathogenesis of human disease states. *Curr. Mol. Med.* 1 (3), 287–296. doi:10.2174/1566524013363816

Yildirim, A., Ozgur, E., and Bayindir, M. (2013). Impact of mesoporous silica nanoparticle surface functionality on hemolytic activity, thrombogenicity and non-specific protein adsorption. *J. Mater. Chem. B* 1 (14), 1909–1920. doi:10.1039/c3tb20139b

Yoshida, T., Yoshioka, Y., Morishita, Y., Aoyama, M., Tochigi, S., Hirai, T., et al. (2015). Protein corona changes mediated by surface modification of amorphous silica nanoparticles suppress acute toxicity and activation of intrinsic coagulation cascade in mice. *Nanotechnology* 26 (24), 245101. doi:10.1088/0957-4484/26/24/245101

Yu, T., Malugin, A., and Ghandehari, H. (2011). Impact of silica nanoparticle design on cellular toxicity and hemolytic activity. *ACS Nano* 5 (7), 5717–5728. doi:10.1021/nn2013904

Yu, X., Liu, T., and Lin, R. (2020). Development and characterization of a glimepiride-loaded gelatin-coated mesoporous hollow silica nanoparticle formulation and evaluation of its hypoglycemic effect on type-2 diabetes model rats. *ASSAY Drug Dev. Technol.* 18 (8), 369–378. doi:10.1089/adt.2020.987

Yu, Y., Duan, J., Li, Y., Li, Y., Jing, L., Yang, M., et al. (2017). Silica nanoparticles induce liver fibrosis via TGF-β$_1$/Smad3 pathway in ICR mice. *Int. J. nanomedicine* 12, 6045–6057. doi:10.2147/ijn.s132304

Yu, Y., Duan, J., Li, Y., Li, Y., Jing, L., Yang, M., et al. (2017). Silica nanoparticles induce liver fibrosis via TGF-β$_1$/Smad3 pathway in ICR mice. *Int. J. Nanomedicine* 12, 6045–6057. doi:10.2147/ijn.s132304

Yuan, S., Liu, H., Yuan, D., Xu, J., Chen, Y., Xu, X., et al. (2020). PNPLA3 I148M mediates the regulatory effect of NF-kB on inflammation in PA-treated HepG2 cells. *J. Cell. Mol. Med.* 24 (2), 1541–1552. doi:10.1111/jcmm.14839

Zaharudin, N. S., Isa, E. D. M., Ahmad, H., Rahman, M. B. A., and Jumbri, K. (2020). Functionalized mesoporous silica nanoparticles templated by pyridinium ionic liquid for hydrophilic and hydrophobic drug release application. *J. Saudi Chem. Soc.* 24 (3), 289–302. doi:10.1016/j.jscs.2020.01.003

Zhang, J., Rosenholm, J. M., and Gu, H. (2012). Molecular confinement in fluorescent magnetic mesoporous silica nanoparticles: Effect of pore size on multifunctionality. *ChemPhysChem* 13 (8), 2016–2019. doi:10.1002/cphc.201100943

Zhang, L., Zeyu, W., Liu, B., Jang, S., Zhang, Z., and Jiang, Y. (2021). Pyroptosis in liver disease. *Rev. Esp. Enferm. Dig.* 113 (4), 280–285. doi:10.17235/reed.2020.7034/2020

Zhang, Q., Wang, L., Wang, S., Cheng, H., Xu, L., Pei, G., et al. (2022). Signaling pathways and targeted therapy for myocardial infarction. *Signal Transduct. Target. Ther.* 7 (1), 78–38. doi:10.1038/s41392-022-00925-z

Zhang, Q., Xu, H., Zheng, S., Su, M., and Wang, J. (2015). Genotoxicity of mesoporous silica nanoparticles in human embryonic kidney 293 cells. *Drug Test. analysis* 7 (9), 787–796. doi:10.1002/dta.1773

Zhang, W., Zheng, N., Chen, L., Xie, L., Cui, M., Li, S., et al. (2018). Effect of shape on mesoporous silica nanoparticles for oral delivery of indomethacin. *Pharmaceutics* 11 (1), 4. doi:10.3390/pharmaceutics11010004

Zhang, X., Luan, J., Chen, W., Fan, J., Nan, Y., Wang, Y., et al. (2018). Mesoporous silica nanoparticles induced hepatotoxicity via NLRP3 inflammasome activation and caspase-1-dependent pyroptosis. *Nanoscale* 10 (19), 9141–9152. doi:10.1039/c8nr00554k

Zhao, J., Qi, Y-F., and Yu, Y-R. (2021). STAT3: A key regulator in liver fibrosis. *Ann. Hepatology* 21, 100224. doi:10.1016/j.aohep.2020.06.010

Zhao, Y., Sun, X., Zhang, G., Trewyn, B. G., SlowingII, and Lin, V. S-Y. (2011). Interaction of mesoporous silica nanoparticles with human red blood cell membranes: Size and surface effects. *ACS Nano* 5 (2), 1366–1375. doi:10.1021/nn103077k

Zhao, Y., Wang, Y., Ran, F., Cui, Y., Liu, C., Zhao, Q., et al. (2017). A comparison between sphere and rod nanoparticles regarding their *in vivo* biological behavior and pharmacokinetics. *Sci. Rep.* 7 (1), 4131–4211. doi:10.1038/s41598-017-03834-2

Zheng, N., Li, J., Xu, C., Xu, L., Li, S., and Xu, L. (2018). Mesoporous silica nanorods for improved oral drug absorption. *Nanomedicine, Biotechnol.* 46 (6), 1132–1140. doi:10.1080/21691401.2017.1362414

Zhu, S., Zhang, J., Zhang, L., Ma, W., Man, N., Liu, Y., et al. (2017). Inhibition of Kupffer cell autophagy abrogates nanoparticle-induced liver injury. *Adv. Healthc. Mater.* 6 (9), 1601252. doi:10.1002/adhm.201601252

Zuo, D., Duan, Z., Jia, Y., Chu, T., He, Q., Yuan, J., et al. (2016). Amphipathic silica nanoparticles induce cytotoxicity through oxidative stress mediated and p53 dependent apoptosis pathway in human liver cell line HL-7702 and rat liver cell line BRL-3A. *Colloids Surfaces B Biointerfaces* 145, 232–240. doi:10.1016/j.colsurfb.2016.05.006

Glossary

MSN	Mesoporous silica nanoparticles
IV	Intravenous
IP	Intraperitoneal
NP	Nanoparticles
SP	Silica particles
nSP	Nano-sized silica particles
GSN	Gelatin-coated mesoporous hollow silica nanospheres
MRT	Mean residence time
AUC_{0-24h}	24-h area under the curve
CMSN	Chiral mesoporous silica nanoparticles
E-CMSN	Enlarged chiral mesoporous silica nanoparticles (E-CMSN)
P NIPAM-co-MAA	N-isopropylacrylamide-co-methacrylic acid
DOX	Doxorubicin
PLMSNs	PEGylated lipid bilayers coated with highly ordered MSNs
RES	Reticuloendothelial system
NLR	Long rod NPs ()
NSR	Short rod NPs
NS	Spherical NPs
A-HMSNs	Albumin-coated hollow MSNs
MSNR	Mesoporous silica nanoparticles
MSNS	Mesoporous silica nanospheres
FMSN-PEG	PEGylated fluorescent MSNs
B-AMSX	Amino-modified mesoporous silica xerogel
B-MSX	Mesoporous silica xerogel without amino modification
MSM	Mesoporous silica microparticles
WMS	Wrinkled mesoporous silica
WMC	Wrinkled mesoporous carbon
SCC25	Squamous cell carcinoma cell line
TA	Trimethylammonium
NF-κB	Nuclear factor-kappa B
TLR	Toll-like receptors
TNF-α	Tumor necrosis factor alpha
IL-6	Interleukin-6
CKD	Chronic kidney disease
ROS	Reactive oxygen species
NO	Nitric oxide
iNOS	Inducible NO synthase
CAT	Catalase
NADPH	Nicotinamide adenine dinucleotide phosphate

NOX	NADPH oxidase
TRPM2	Transient receptor potential melastatin 2
HEK293	Human embryonic kidney 293 cell line
Nrf2	Nuclear factor erythroid 2-related factor 2
HO-1	Heme oxygenase 1
JAK2/STAT3	Janus kinase 2/signal transducer and activator of the transcription 3
IP15	Glomerular mesangial cells
MDCK	Epithelial distal tubular cells
PK 15	Porcine kidney
NRK-52E	Rat kidney cell line
FOXO3	forkhead box protein O3
KC	Kupffer cells
PPARγ	Peroxisome proliferator-activated receptor gamma
HSC	Hepatic stellate cells
TGF-β	Transforming growth factor-β
NLRP1	Nucleotide-binding oligomerization domain-like receptor protein 1
IL-18	Interleukin-18
AST	Aspartate aminotransferase
ALT	Alanine aminotransferase
G6PD	Glucose-6-phosphate dehydrogenase
HK	Hexokinase
PEK	Phosphofructokinase
TCA	Tricarboxylic acid
GSSG	Glutathione disulfide
$NADP^+$	Nicotinamide adenine dinucleotide phosphate
PEG	Polyethylene glycol
RBC	Red blood cells
WBC	White blood cells
PT	Prothrombin time (PT)
aPTT	Activated partial thromboplastin time
DOE	Design of experiment